Centrifuge 98, Kimura, Kusakabe & Takemura (eds) © 2000 Balkema, Rotterdam, ISBN 90 5809 000 0

NECER: Network of European Centrifuges for Environmental Geotechnic Research

J.Garnier & L.Thorel – *Laboratoire Central des Ponts et Chaussées, Nantes, France*

R.Lynch, M.Bolton, C.Kechavarzi, A.Treadaway, H.Coumolos & K.Soga – *University of Cambridge, UK*

D.König, A.Rezzoug & G.Heibrock – *Grundbau und Bodenmechanik, Ruhr-Universität Bochum, Germany*

F.A.Weststrate, J.T.Van der Poel, O.Oung & R.R.Schrijver – *Delft Geotechnics, Netherlands*

R.N.Taylor, S.Robson & S.Spiessl – *City University, London, UK*

H.G.B.Allersma & G.M.Esposito – *University of Delft, Netherlands*

M.Davis & S.Burkhart – *University of Cardiff, UK*

C.M.Merrifield & W.H.Craig – *University of Manchester, UK*

ABSTRACT: Geotechnical environmental problems related to contaminant transport in soils are gaining increasing importance with the implementation of new policies on waste disposal and with problems of restoration of polluted areas. Centrifuge modelling may be of special interest to provide a correct understanding of pollutant transport and to validate numerical models but it requires the knowledge of scaling relations and the development of special sensors. The NECER project (Network of European Centrifuges for Environmental Geotechnics Research) is funded by the European Union and involves the cooperative efforts of eleven institutes. The report presents the organisation and the aim of the NECER network and the work in progress within the different working groups.

I ORGANISATION AND AIM OF THE NETWORK

J. Garnier, LCPC, France

Up to now, the most fruitful applications of centrifuge modelling have been in the field of geotechnical engineering and soil/structure interactions. However, in most countries there is an increasing concern with environmental soil related problems (contaminant transport, waste containment, soil cleaning) and centrifuge modelling seems to be a valuable tool in these domains (Arulanandan et al 1988, Cooke & Mitchell 1991, Li et al 1994, Mitchell R.J. 1994, Villar et al 1994, Culligan-Hensley & Savvidou 1995). However pollutant transport processes are complex because they are often driven simultaneously by different phenomena (convection, mechanical dispersion, molecular diffusion) and many scaling conditions have still to be investigated (Peterson & Cooke 1994, Knight & Mitchell 1996, Penn et al 1996, Culligan et al 1997). Much remains to be done to bring physical modelling to the same level as for more classical soil/structure interaction problems and international cooperation is obviously needed.

The European Union funded network NECER - Network of European Centrifuges in Environmental Geotechnics Research - was set up in 1996 under the coordination of J. Garnier. The network consists of eleven European research institutions, both academic and industrial, whose aim in this project is to carry out joint research on civil engineering environmental topics using centrifuge technologies, and in the process to train researchers.

In order to develop the capabilities of centrifuge modelling in environmental engineering and to assess its limits, a limited number of topics has been selected to form the scientific programme of the project (Table 1).

Table 1. Basic tasks and working groups

WG A	WG B	WG C
Development of sensing and imaging for detection of contaminant migration	Capillary phenomena and problems of pollutants transport in non-saturated soils	Non aqueous phase liquid pollutant migration (LNAPL and DNAPL)

The current participations of the NECER partners in the different working groups are shown in table 2.

Table 2. Partners participation in the different working groups

NECER partners	WG A	WG B	WG C
LCPC (FR)	x	x	
Cambridge Univ. (GB)	WG leader	x	x
Bochum Univ. (DE)	x	WG leader	
Delft Geotechn. (NL)	x		WG leader
City Univ. (GB)	x		x
Cardiff Univ. (GB)	x	x	x
Delft Univ. (NL)	x		x
Manchester Univ. (GB)	x	x	
LNEC (PT)	x	x	
Danish Tec. Univ. (DK)		x	
ISMES (IT)	x		x

A fourth working group, under the direction of LCPC, has been organised to coordinate the training activities of the network and five actions are engaged:

Action 1: Maintenance and diffusion through the Web of a large international data base of references on centrifuge work publications.
Action 2: Production of short videos from actual experiments.
Action 3: Training of permanent staff of centrifuge teams.
Action 4: Training of young researchers by stays among foreign teams (160 man-month salaries are provided by the network).
Action 5: Organisation of an international symposium on the application of physical modelling to environmental geotechnics (NECER 2000).

This International Symposium on Physical Modelling and Testing in Environmental Geotechnics will be held in La Baule (France) from 15 to 17 May 2000.

The following sections presents the works under progress within the three technical working groups.

II DEVELOPMENT IN SENSING AND IMAGING

R.Lynch, Cambridge University, GB

Part of the research of the programme is aimed at providing information about the mobility of pollutants in soils. This section describes recent work to develop novel devices or imaging systems to track the movement of pollutants, in both 1g and in high g centrifuge experiments.

1 CHEMICAL SENSORS

1.1 In-situ fibre-optic photometric sensing

A C J Treadaway, M D Bolton and R J Lynch

For the monitoring of inorganic contaminants the use of resistivity probes has proved invaluable. However for organic contaminants, an alternative to resistivity probes may be required, and work at Cambridge University, and later at LNEC Lisbon by H. Barker, M.G. Silva and J. de Almeida Garrett made use of the property of light absorbance of the pore fluid, since this can be easily related to measure organic compound concentration. Light is carried by fibre optics to small cells buried in the soil, in which the optical absorbances of the pore fluid are measured (Treadaway 1997, 1998). Light exits from the cell by another fibre which transmits light to a photodiode.

A typical photometric sensor cell is shown in Figure 1 The device itself is about 10mm in diameter. A number of these devices may be buried in the soil to record the passage of a plume of pollutant. Figure 2

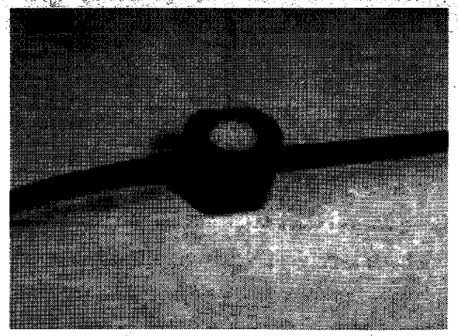

Figure 1. A fibre-optic photometric sensor cell.

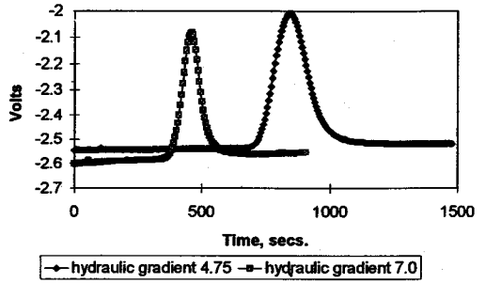

Figure 2. Downward moving plumes under different hydraulic gradients, recorded by a photometric sensor buried in the soil.

shows the vertical plumes moving under different hydraulic gradients recorded by a buried photometric sensor, in which the plumes resulted from spillages of dye on the soil surface.

When a similar experiment is mounted in a centrifuge, pollutant transport advection is increased by the high gravitational field, and the accelerated breakthrough time and the shape of the plume can be measured.

Figure 3 shows the preliminary result from a centrifuge experiment where green dye was spilled as a pollutant on to water-saturated fine sand. The sand is contained in a 200mm diameter cylinder in which the two sensors were buried at 46 and 86 mm from the surface. A constant water head of 10mm above the surface was maintained electronically. Water and dye reservoirs are alternately switched on remotely by solenoid valves. The passage of the green dye tracer is shown in Figure 3. The profile of the plume provides information about the dispersion as it passes vertically through the soil.

Also the linear velocity of the pore fluid can be calculated from the difference in sensor traces.

In future it is intended to use a sand / clay / sand barrier with a sensor placed on either side of the clay.

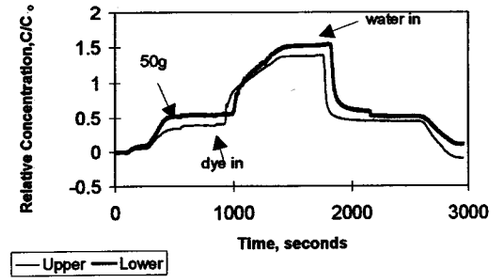

Figure 3. Green dye plumes observed during a 50g centrifuge test.

In this way we hope to determine the breakthrough time which will be controlled by the retention of the dye by the clay.

1.2 Ion selective electrode

F.A. Weststrate and R.R. Schrijver

For the research on the sorption behaviour of contaminants by 1g or ng column-experiments, it is required to follow the breakthrough of the specific contaminant. By measuring the concentration in time in the outflow, the so-called breakthrough curve can be constructed. In this way information is obtained on the retardation of the contaminant of interest, compared to the breakthrough of a non-sorbing compound.

There are different methods to obtain the breakthrough curve. One is to sample the outflow in time and analyse the samples for the contaminant, the other method is to measure the concentration online. The last method requires a detection system that is only sensitive to the contaminant of interest. For the online detection of some (heavy) metals use can be made of ion selective electrodes, in our case a copper selective electrode. The ion selective electrode is used in conjunction with a reference electrode and the measured potential is proportional to temperature and log activity according to the Nernst equation. The relation between concentration and activity is:

$$a = f.c$$

where a is the activity of the ion to be measured, f is the activity coefficient and c is it's concentration. The activity depends on the ionic strength of the solution and equals one if the ionic strength equals zero, so in dilute solutions concentration equals activity and the concentration can be measured directly. Before the experiments, the electrode has to be calibrated. From the calibration curve (Figure 4) the concentration can be found.

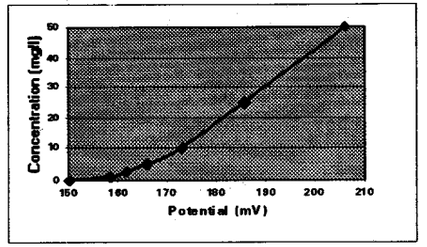

Figure 4. Calibration curve for Copper.

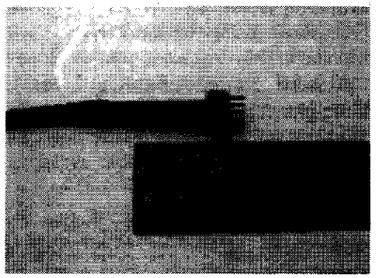

Figure 5a Resistivity probe.

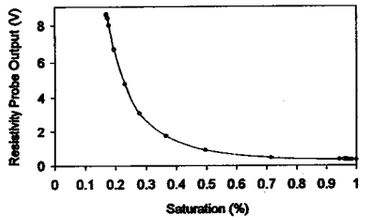

Figure 5b. Resistivity calibration curve.

At Delft Geotechnics the ion selective electrode is used for the research on sorption kinetics. For the online measurement a flow cell, in which the electrodes are mounted, is used.

2 WATER CONTENT AND FLUID PRESSURE

2.1 Water content and fluid pressure measurement using resistivity probes and tensiometers

C. Kechavarzi and K. Soga

When LNAPL (Light Non Aqueous Phase Liquid) is released in the unsaturated zone, three fluid phases are present (water-LNAPL-air). In order to solve the governing equations describing immiscible multi-phase flow and to investigate NAPL behaviour in the centrifuge, knowledge of the constitutive relations among fluid relative permeabilities, saturations and

pressures is required. In this research water saturation is measured using resistivity probes (Figure 5a) which, in the past, have been used as a standard tool to monitor ion migration in the centrifuge (Hensley 1989). This can be achieved by using water of known conductivity (Nacl solution) and a non-conductive NAPL. When water saturation decreases the resistivity of the system increases (Figure 5b).

It is intended to estimate NAPL saturation using image analysis techniques (Van Geel and Sykes 1994). By continuity the air saturation is deduced from water and NAPL saturation.Water and NAPL negative pressures are measured using tensiometers, which consist of hydrophilic and hydrophobic porous stones connected to pressure transducers (Figure 6a-b). Usually, in a three-phase system, the air phase is in contact with the atmosphere and the air pressure remains atmospheric.

2.2 High frequency capacity probe for water content measurements

J. Garnier, L. Thorel

Electric methods are used for years for measuring water content in civil engineering materials. Capacity probes are based on the difference in dielectric constant of water (ε'=80) compare to solid (ε'=3 to 5) and air (ε'=1). The frequency must be high enough to avoid polarisation phenomena and to reduce the effect of electric conduction. LCPC has developed a high frequency probe working in the range 30-50 MHz for use in aggregates, concrete, soil and walls.

A first series of smaller probes has been built for measuring water content in columns during centrifuge tests (figure 7). These sensors are installed outside the column and the electrodes are introduced into the soil sample through the wall. For a correct transmission of the output signals to the control room through the sliprings, an electronic printed circuit including a frequency divider is placed in the sensor as close as possible to the electrodes.

More recently, to allow water content measurements in much larger centrifuged samples, a miniaturised probe that could be totally embedded into the soil has been developed. The sensor is 4 cm long and 2 cm in diameter and the two electrodes are placed along the cylindrical body. The in flight calibration of such sensors is not possible since the water content in the centrifuged model is unknown. It was decided to operate in two stages:

-1 g calibration tests in different soils. The water content used as reference is measured by weighting continuously the sample during the tests. The relationships between the measured frequency F and water content w are as follows (Dupas et al 1995):

$\Delta F/\Delta w$=3700 Hz in sand $\Delta F/\Delta w$=2500 Hz in silt

-Study of the effects of accelerations on the sensors. In these tests, the probe is embedded in dry Fontainebleau sand with a constant and near zero water content. Results of 1g-100g tests are plotted in figure 8. The observed change in frequency due to increase in acceleration from 1g to 100g is only ΔF=5 Hz. This spurious response would lead in wet soils to an error in the measured water content less than Δw=0.2 %. Figure 8 shows no significant shift in the probe response during the 15 mn rotation at 100g.

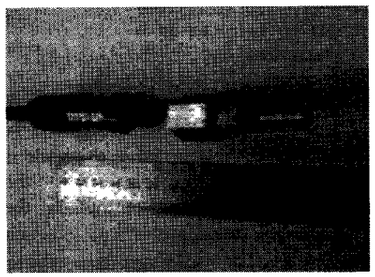

Figure 6a. NAPL and water tensiometer.

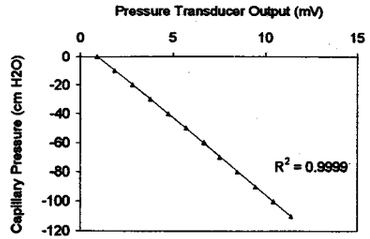

Figure 6b. Tensiometer calibration.

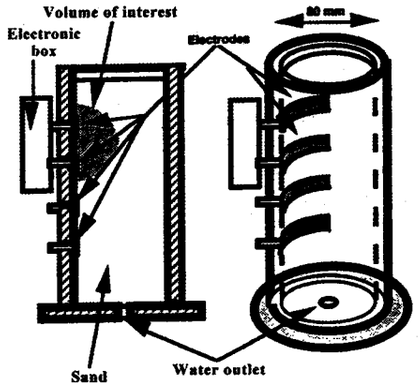

Figure 7. Centrifuge columns with high frequency probes

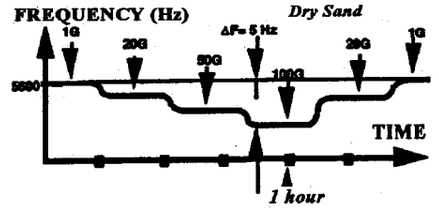

Figure 8. Effect of the centrifuge acceleration on probe response

To install this water content probe in the LCPC centrifuge CPT device, its diameter is now being reduced to 12 mm.

2.3 Moisture content measurement by radioactive tracers

C M Merrifield

Preliminary tests have been undertaken to demonstrate that the moisture content of a partially saturated fine sand may be predicted using Technetium-99m as a radiotracer within a dilute solution of Sodium Pertechnetate as solute. The development of this technique will facilitate the determination of the moisture content in the vadose zone in-flight during the investigation of capillary phenomena in the centrifuge.

To date the moisture content in columns of sand subjected to capillary rise in the centrifuge has been determined by standard moisture content tests on samples retrieved after the test has been concluded. This method has suffered from inherent inaccuracy due to moisture content redistribution during spin-down and time taken to sample the soil at the required locations within the column.

Moisture content determination by monitoring the level of radioactivity of a very dilute solution of a weakly sorbing radioisotope allows the accurate observation in real time of the movement of the moisture during capillary rise in a centrifuge test. Combining this with the measurement of soil suction at precise locations in the soil column allows the development of a matric suction curve in real time during the test.

The activity of the radiotracer was measured by miniature Geiger-Mueller tubes type AG1300. These are Halogen quenched γ and high energy β (0.5MeV) radiation counter tubes.

The Geiger tubes can operate in virtually any environment, being unaffected by variations in water chemistry, light intensity, temperature or gravitational forces. (Villar, 1993; Villar et al, 1994) Their small size and flexibility facilitates manipulation and placement within a test rig. Suitably encapsulated the tubes can withstand water pressures in excess of 500kPa.

The measurements from the detectors are corrected for decay, concentration of the radiotracer and voids ratio. A linear relationship between a weighted count rate and the insitu moisture content has been found from initial tests as shown in Figure 9. The tests have demonstrated the suitability of using a radiotracer to monitor moisture content in a partially saturated sand.

The technique requires careful calibration of the detectors and establishment of the parameters which affect the count rate during the test. These are: (a) soil density, (b) soil type, (c) initial activity level of radiotracer, (d) concentration of radiotracer in the solution, (e) degree of detector collimation, (f) ion exchange capacity of the solid phase.

3 IMAGE PROCESSING

3.1 Using digital image processing in monitoring LNAPL infiltration in sand.

H.G.B. Allersma

Digital image processing can be considered as a universal tool to visualise and digitise phenomena in geotechnical experiments. The optical measuring technique is introduced in centrifuge research by Allersma (1990), Corte and Garnier (1992) in order to perform detailed deformation measurements in small models. It soon appeared, however, that there were many more applications in experimental geotechnics, as well as in the laboratory as in field tests (Allersma, 1997). A recent development is the use of image processing in monitoring pollution transport phenomena in centrifuge test. The contours of the spill in a two dimensional tests as well as the concentration of the contaminant over the area of the plume can be digitised.

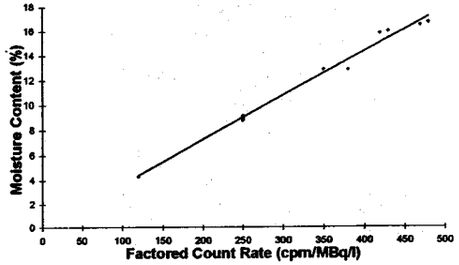

Figure 9. Relationship between moisture content and factored count rate.

The image processing system used comprises a PC with a frame grabber and a CCD camera. By sending commands to the frame grabber video images can be captured and stored on disk. For elaboration of the images it is recommended to use a toolkit. Several toolkits are on the market. The software supplies the user with a large amount of commands, which can be used to extract significant information from the images.

Digitisation contour LNAPL plume

The contaminated area in a two dimensional test is visible thanks to black paint which is added to the NAPL. The extraction of the NAPL plume from the background is based on differences in grey value. To prevent the appearance of non-significant objects a subtraction can be performed between the initial stage and the actual image. Objects which are not changed in time are removed. A typical result of this operation is shown in Figure 10a. Next the plume area can be extracted by a threshold command, which means that only grey values within a specified range are left. Only one object is now left (Figure10b).

The number of pixels in the object can be counted and be used to calculate the surface. The toolkit provides a command which draws a frame around the object, so that the extreme co-ordinated of the plume are known. Furthermore the boundary of the plume can be digitised by a single command.

In Figure10c some digitised stages are plotted in the original image. By subtracting two test stages the expansion of the plume in time can be measured. Since the NAPL level in the supply container can also be measured by image processing oil supply can be compared with the plume grow. In the first instance the geometry is derived in image pixels. By placing markers on the transparent wall at known distances the image pixels can be converted easily into metric units. If an area of 100x150 mm is monitored displacements can be measured with an accuracy of 0.3mm.

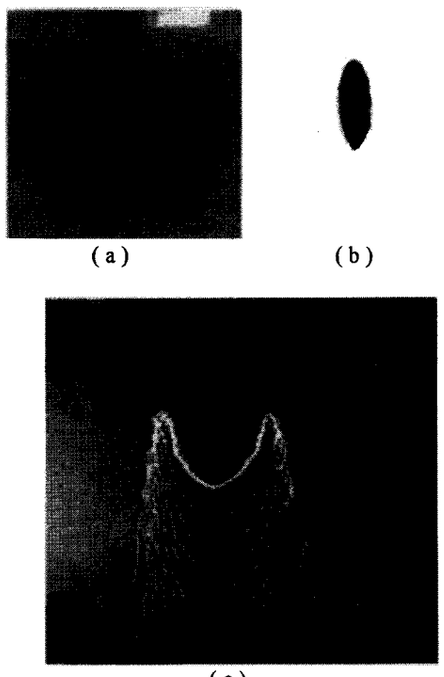

Figure 10 (a) Subtraction, (b) Threshold, (c) Contour.

Concentration measurement

Information about the NAPL concentration over the plume area can be obtained using the grey value distribution. In the first instance the plume is located and isolated using the information obtained in the previous chapter. Next the plume is scanned by small sub frames, where in each sub frame the averaged grey value is determined. A special option makes it possible to neglect the background at the boundary of the plume, so that also here good averaged values are obtained. The measurement can be performed after well defined time intervals and stored in a file. The grey value can be linked to a concentration by calibration. Well known mixtures of sand and NAPL can be made, where the grey value is measured. It is also possible to measure the NAPL concentration at some locations in the test model afterwards. In the beginning of the test the sand is fully saturated, so that in this stage also a reference point is obtained.

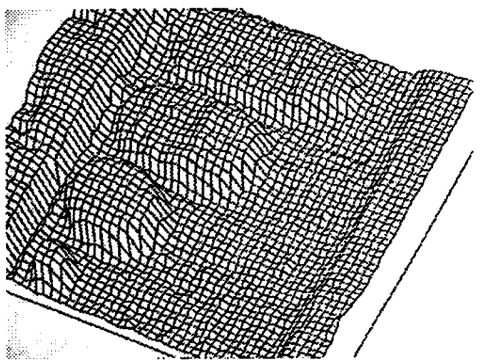

Figure 11. Three dimensional plot of the NAPL concentration distribution over the plume in four test stages.

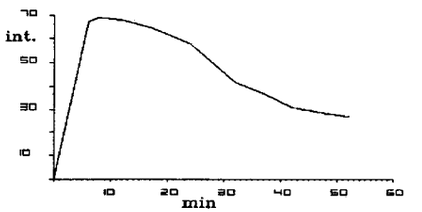

Figure 12. Measured grey value in time at some location.

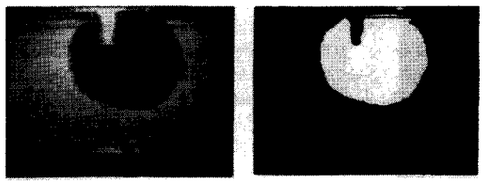

Figure 13. (a) Digital image of centrifuge model test showing DNAPL plume (white mark at top of figure is a reflection of the light source); (b) limits of DNAPL plume following analysis of images.

In Figure 11 the concentration distribution in four stages of the test is shown in a three dimensional plot. The full saturation can be observed in the first instance, where in a later stage the concentration decreases.

In Figure 12 the course of the concentration in time is shown at some point close to the surface of the sample. The sudden appearance of the NAPL during injection is shown, where the concentration decreases gradually after the injection has been stopped. The NAPL concentration ranges approximately between 7 % and 14 %.

Digital image technology can be used to perform measurements in two dimensional pollution transport tests. Only a camera is needed as sensor and light is not influencing the test. The following parameters can be measured: dimensions plume, velocity infiltration, area plume and local concentration of NAPL in plume.

3.2 Image analysis applied to centrifuge model tests of environmental engineering problems

R.N. Taylor, S. Robson and S. Spiessl

A key part of the NECER project is to evaluate the possibility of modelling DNAPL flow in saturated soils using centrifuge testing techniques. The migration of a plume of DNAPL, i.e. a pollutant immiscible in water, can be characterised simply by its advancing front provided the assumption can be made that there is insignificant mixing or entrapment of water as the DNAPL plume passes through the soil. Thus, for plane (2D) flow, the visual sighting of the plume of DNAPL through the side window of a centrifuge container can give considerable information regarding the migration of DNAPL. Analysis of images of models obtained during centrifuge flight is able to provide this information. Of course the assumption that the flow is planar is essential to the success of the method, but if the assumption was found to be in error, then a substantial amount of other related environmental engineering research would be put in doubt, and this in itself would be a valuable result.

At City University over the past 3 years a considerable amount of research has been undertaken to utilise image analysis for the determination of ground movements in geotechnical centrifuge model tests (Taylor et al, 1998). Purpose written software has been developed to enable high accuracy calibrated ground movements to be determined from analysis of the (geometrically distorted) images obtained from on-board miniature CCTV cameras. The system makes use of tracking of discrete targets located on the face of a centrifuge model and coordinates of the targets in the object space can be calculated.

For the DNAPL tests, different techniques of tracking are needed, and in the first instance, consecutive images of the centrifuge tests can be subtracted to eliminate background information, the difference then being only the movement (in pixels in image space) of the front of DNAPL during the elapsed time period between the two images. The techniques of camera and system calibration developed previously can then be used to convert the pixel data into real coordinates in the object.

Figure 13a shows a typical image of a (dark) DNAPL plume advancing in saturated soil model, and Figure 13b shows the plume identified as a solid white area against a black soil background; this was determined essentially by image subtraction. The edge of the advancing plume can then be identified.

Work is in hand to standardise the procedure of calculating the location in object space of the advancing plume and hence for example obtaining the area (volume) of DNAPL flow at any particular time.

III CAPILLARY PHENOMENA IN CENTRIFUGE TESTING *D. König, RUB, Germany*

1 INTRODUCTION

The capillary movement of water through soils is of

interest in many practical environmental engineering problems, and in problems concerning pollutant transport in soils. This section presents the first NECER's results of centrifuge tests on water capillary rise in soils. The main question is to verify scaling laws using different types of soils in different samples with different boundary conditions.

2 THEORETICAL AND EXPERIMENTAL APPROACHES ON CAPILLARY RISE IN CENTRIFUGE MODELLING

G. Heibrock, A. Rezzoug

2.1 Theoretical analysis

The capillary pressure (difference between pressures in both sides of a meniscus) in a cylindrical tube with radius $r = d/2$ [m] is described in Schubert 1982 as :

$$p_c = \frac{2\gamma_0 \cos\delta}{r} f(B_0, \delta) \qquad (1)$$

where γ_0 is the surface tension [N/m] and δ is the contact angle between wall and water[°].
The function f is tabulated by Padday 1969 and it takes into account the possible effects of external fields (gravity). It depends on the Bond number $B_0 = g(\rho_w - \rho_a)d^2/\gamma_0$, where d is the radius of the bottom of the meniscus. The Bond number is then the ratio between body forces over surface tension. Assuming a spherical shape of the boundary surface between water and air, the capillary pressure derived from the Young-Laplace equation under atmospheric pressure is then:

$$p_c = \frac{2\gamma_0 \cos\delta}{r} = g(\rho_w - \rho_a)h_c \qquad (2)$$

where g [m/s^2] is the gravity, ρ_a [kg/m^3] the density of air, usually neglected, ρ_w [kg/m^3] is the density of water, and h_c [m] is the capillary rise. Therefore capillary rise can be calculated from the well know Jurin equation:

$$h_c = \frac{2\gamma_0 \cos\delta}{g(\rho_w - \rho_a)r} \qquad (3)$$

A spherical shape of the surface between water and air (meniscus) can be assumed if (Schubert 1982) :

$$|h_c| >> \left|\frac{r(1-\sin\delta)}{\cos\delta}\right| \qquad (4)$$

This condition corresponds to high surface tension (compared to body forces) and to Bond number much smaller than 1. In this case equation (1) reduces to (2) and in a perfectly wetting fluid (4) reduces to

$$|h_c| >> r \quad \text{or} \quad Bo << 1 \qquad (5)$$

If we assume that capillary rise in soils can be described by the capillary pipe model, equations (2) and (3) are the basis of the scaling laws concerning the flow of water in unsaturated soils. Capillary rise is then scaled down by N under an acceleration of N times the earth gravity.

It is also assumed that in fine sandy soils the representative pore size may be d_{10} ranging from 0.02-0.6 mm. In this case, capillary rise at 1g from equation (3) ranges from 1,47 to 0,05 m, (with γ_0=0,072 N/m at 20°C and d=0). Therefore, the influence of gravity can be neglected for a sand with d_{10} = 0,6 mm. In this case at 1 g conditions equation (5) gives $r = d_{10}/2 = 0{,}3\ mm << h_c = 50\ mm$. But under Ng conditions with N=50, h_c may be reduced by N and is then h_c = 1mm. In this case, r is close to h_c and (5) is not fulfilled.

Schubert 1982 shows that the gravity has also an influence on the shape of water bridges between particles in static condition. This influence can be neglected if

$$\frac{(\rho_w - \rho_a)gd}{|p_c|} < 10^{-2} \qquad (6)$$

This criterion can be applied to water bridges at accelerated g-levels. Schubert (1982) shows that capillary pressure in water bridges follows

$$\left|p_c \frac{d}{\gamma_0}\right| \geq 2 \qquad (7)$$

The geometrical parameter d represents the dimension of the water bridges and it can be assumed that d is smaller than the particle size. The equation (6) holds for particles smaller than 380 µm for water at 1g conditions. From Petersen & Cooke 1994, particles have to be smaller than 380/N$^{1/4}$ µm at Ng. This condition may be too conservative but the latter show that even in fine sands, a 50g acceleration has a significant influence on the capillary pressure of entrapped water. Therefore from a theoretical point of view the simple scaling law does not hold. This means that water remaining entrapped at 1 g may be removed at Ng. On the other hand the influence of gravity can be neglected even at high g-levels for clayey soils with characteristic pore sizes smaller than 1 µm.

In static conditions we assume that the relationship between water content and capillary pressure is unique. This may not be true in dynamic conditions if capillary pressure becomes a function of velocity. If the meniscus in a capillary pipe is moving at a velocity v, the dynamic contact angle $\delta = \delta(v)$ differs from the static contact angle and capillary pressure differs. The dynamic contact angle may depend on the direction of movement resulting in differences between wetting and drying processes. Up to now it is very difficult to measure dynamic contact angles. According to Schubert 1982 the influence of dynamic effects is larger in wetting experiments than when draining conditions occur.

2.2 Previews experimental studies

Scaling relations for unsaturated soil conditions have been studied by Goodings 1984 and Arulanandan & al. 1988. They all assume that same soils and same fluids are used in model and prototype. Thus the characteristic microscopic length of the soil d_{10}, the density of the fluid ρ_w, and the surface tension γ_0 at the fluid-particle interface (which seems not depending from g-level) are the same in prototype and model. Capillary rise at Ng is then scaled down by N, in agreement with equation (3) when the influence of the gravity on the shape of meniscus is neglected.

Most of the works on unsaturated soils are based on these scaling relations (Goforth & al. 1991, Illangasekare & al. 1991, Cooke & Mitchell 1991a&b, Mitchell & Cooke 1991, Mitchell & Stratton 1994, Mitchell 1994, Cooke 1994, Sills & Mitchell 1995, Knight & Mitchell 1995). Most of the publications deal with the verification of the scaling laws by modelling of models tests or by comparison between centrifuge model tests, 1g tests and numerical analysis.

A discussion of the validity of scaling laws has been presented by Petersen & Cooke 1994 but their negative conclusions have been contested by Knight & Mitchell 1996. For applications of centrifuge modelling to unsaturated flow problems (e.g. Radnam & al. 1996) it is important to study these points more in detail using the modelling of models technique.

3 DESCRIPTION OF THE TESTS

D. König, A. Rezzoug

3.1 Introduction

To investigate the influence of the g-level on capillary rise, first tests from dry to wet conditions have been carried at LCPC (France) and in the Universities of Manchester (UK), Cardiff (UK) and Bochum (Germany). The concept of the test has been the same in all laboratories, but boundary conditions may differ due to differences in the equipment.

3.2 Test design and measurement techniques

The devices are described in Figure 1 and in Table 1.

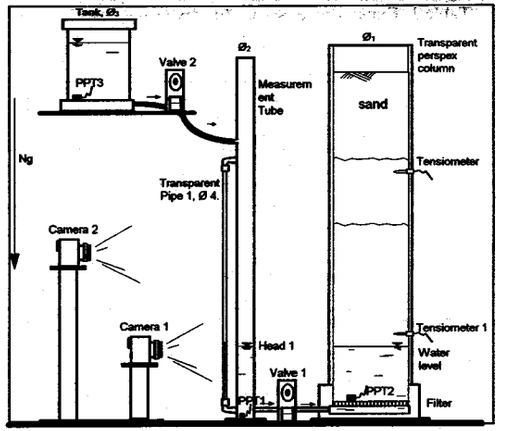

Figure 1. Common basic scheme (from Bochum device).

A sand sample is prepared in a transparent column with an internal diameter $Ø_1$, using raining methods. Water is introduced in flight at the bottom of the column through a measurement tube (diameter $Ø_2$). In the Bochum equipment, water is provided to the measurement tube from a tank (diameter $Ø_3$) through valve 2. Connection between the tub and the column is controlled by valve 1.
Different measurement techniques are used:
• Pore pressure transducers (PPT) : they are placed in the sand sample to record pore pressures or in the tubes and tanks to monitor the height of water.
• Tensiometers : In Cardiff tests, Tensiometer 1 & 2 are used to measure suction in the sand above the phreatic surface (Figure 1).
• Video Camera : one or two cameras are placed on the model to follow displacements of the wet front in the sand inside the transparent column.

3.3 Test procedure and programme

The centrifuge is accelerated at the selected g level and valve 1 is opened (Figure 1). Water flows from the measurement tube into the sand sample. The water table rises in the sand and falls in the measurement tube until equilibrium is reached when the hydraulic gradient has dropped to zero.

Concerning the test procedures in different laboratories the following details are pointed out:

• In Manchester where the centrifuge has a fixed arm rotor a slightly different system is used. A constant head arrangement consists of a tank and an over flow device being continuously supplied with water from off centrifuge. This has the advantage that flow under hydraulic gradient to establish the phreatic surface is nearly complete before the onset of capillary rise.

Table 1. Experimental set-up for dry to wet tests.

	Manchester	Bochum	Cardiff	LCPC
Sand d_{10}/d_{50}[mm]	HPF5 : 0,05/0,2 PFA : 0,02/0,07 Congleton 0,1/0,15	Bochum normsand 0,12/0,18	Congleton 0,1/0,15	Fontainebleau 0,15/0,2
Sand Column Diam. $Ø_1$/height [m]	0,04/0,5 Perspex column	0,2/1 Perspex column made by superposable transparent rings (height variable up to 1m)	0,18/1 Perspex Column	Rectangular container with glass wall 0,8/0,4/0,36
Measur. tube $Ø_2$ [m]	Over flow system (Tank)	0,045	0,18	Mariotte bottle
Centrifuge radius to platform	3,2m Fixed platform	4,125m Swinging basket	2,582m Swinging basket	5,5m
Depth of applied g-level	At phreatic surface in the sand	At phreatic surface in the sand	At one third of the sand column height	At water table level (Mariotte bottle)
Model Preparation	Pluviation followed by densification (knocks on column wall)	Pluviation	- Pluviation - Deaired water and inner coating with hydrophobic lubricant	Pluviation by automatic hopper
Calibration of PPT and Tensiometer	/	During flight at increasing g-levels	1g before the tests	1g before the tests
Test programme (g-level)	HPF5: 45, 30, 20, 10, 1g PFA: 100, 60, 30, 25, 12,1g	40, 20, 10, 1g	1st test: 30, 20, 10, 5g 2nd test: 10, 7, 5, 3, 2, 1g	Tests at 1, 6, 20, and 40g
Test Procedure	- Valve opened at Ng. New sample for each test. - Constant phreatic surface (over flow system)	- Valve opened at selected g-level from initial state in dry sand - New test for each chosen g-level	- Valve closed between two successive g-levels. - Continous test decreasing g-levels step by step	Dry to wet and wet to dry tests Constant water table (Mariotte bottle)

• In Bochum the tests start with an initial water level in the measurement tube. During the increase in acceleration, PPT's are recorded and measurements are used for the transducers calibration. At the chosen g level, valve 1 is opened (time t = 0). At equilibrium, water table level is assumed to be the same in the column and in the measurement tube. The effect of the variable gradient between measurement tube and column is neglected.

• In Cardiff, the two series of tests consisted in transferring the dyed water from the measurement tube into the sand column by opening the valve 1 when the selected g-level has been reached. At equilibrium, the valve is closed during the time to decelerate the centrifuge to the next g level and the procedure is repeated. The amount of water involved in the fringe itself is derived from the water table height.

Tensiometer 1 is placed just above the initial equilibrium level (before the fringe started) and registers directly the change in suction (negative pressures above water table) due to the fringe development.

Tensiometer 2 is installed in dry sand during the tests. Only the part of the fringe hydrostatically connected (continuous phase) is measured there.

• In LCPC, a system based on a Mariotte bottle is used to keep the water table level constant in the measurement tube during the whole centrifuge test. The sand sample is previously pluviated in a large rectangular container with a transparent wall (L=0.8 m, l=0.4 m and h=0.36 m). As the equipment is different from the three others (large rectangular container instead of cylindrical column), results of these tests are not reported there.

4 MANCHESTER TEST RESULTS

W.H. Craig

The movement of the wetting front has been observed by video cameras over periods up to 8 hours in the finer and less permeable PFA, for which the rise at 1g is on the order of 6m over many months. The somewhat coarser HPF5 sand has a rise of amount 3 m at 1g. Tests in both materials over a range of accelerations up to 60g confirm the N scaling of capillary rise, with N^2 scaling of time of rise as shown in Figure 2 in which the prototype rise is expressed as N x (observed model rise), Mitcheson 1997. Some anomalies at higher accelerations are currently attributed to experimental difficulties and will be investigated further. Figure 3 presents the same results in logarithmic scale.

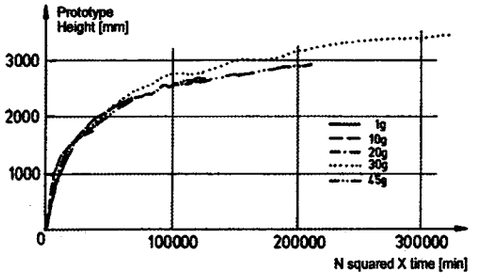

Figure 2. Capillary rise vs time in HPF5 sand under accelerations ranging from 10 to 45g (Manchester).

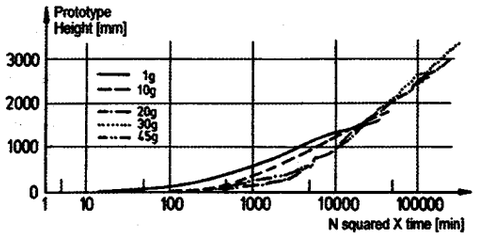

Figure 3. Capillary rise in HPF5 sand in logarithmic scale (Manchester).

5 BOCHUM TEST RESULTS

D. König, A. Rezzoug

5.1 Results of optical measurements

The capillary wet front is defined as the visible frontier between dry sand with its initial colour, and wet darker sand. The capillary rise is the distance from the water table to the capillary wet front level in the sand.

In the following figures, capillary rise is plotted versus time or versus g-levels. Each curve represents one centrifuge test performed on one sand sample. Letters M or P placed as exponent indicate model or prototype values.

Figure 4 shows the result in prototype dimensions of four tests carried out at 1, 10, 20 and 40g. The scale factors used are 1/N for capillary rise h_c and N^2 for time. The 1g test is well simulated by the centrifuge tests in term of final capillary rise.

For the earlier stage of the 40g test, the agreement is not so good. The model time has been multiplied by N^2=1600 and the rise h_c by N=40. The poor accuracy of the first readings is perhaps the reason of the observed discrepancy. Dynamic effects and superposition of water flow due to hydraulic gradient and due to capillarity may also have influenced the results in the first stage of the 40g test.

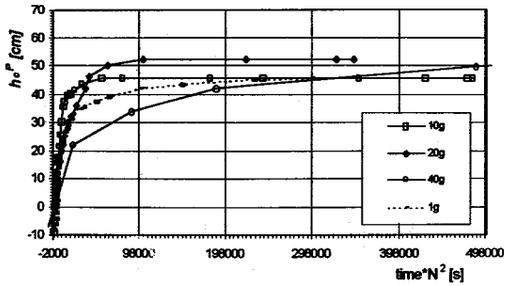

Figure 4. Prototype visual capillary rise versus time scaled by N^2 (Bochum).

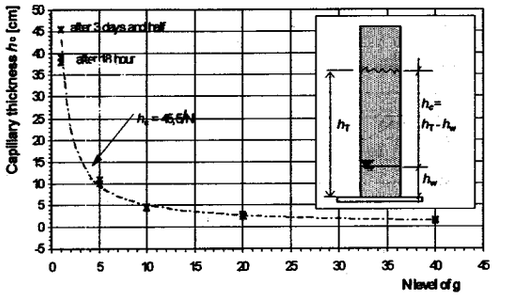

Figure 5. Optical measurements of final model capillary rise versus acceleration (Bochum).

Figure 5 gathers results of optical measurement on final capillary rise versus g-level and shows that h_c follows the 1/N similitude law. For the 1g-test, it was rather difficult to locate precisely the wet front position after 3 days.

The good agreement between tests results is confirmed in Figure 6 where all prototype values of final h_c are very similar for acceleration ranging from 1g to 40g.

5.2 Results of volume measurements

The volume of water V_c hold by capillarity in the sand may be calculated from the measured height of water in the tube and in the saturated part of the sand sample. If total volume of water transferred into the sand sample is V_T and the volume of water in the saturated sand is V_w, then V_c can be estimated by $V_c = V_T - V_w$.

Total volume V_T and volume of capillary water V_c are plotted in Figure 7 versus acceleration. The data for V_c are well fitted by the curve $V_c = V_c^{1g}/N = 3490cm^3/N$. As the section of the sand sample is always the same in all tests, this means that the capillary rise is well scaled by the factor N.

In Figure 8 the volume V_c measured in each test is multiplied by N giving the prototype value V_c^P. A slight increase of V_c^P with acceleration is observed

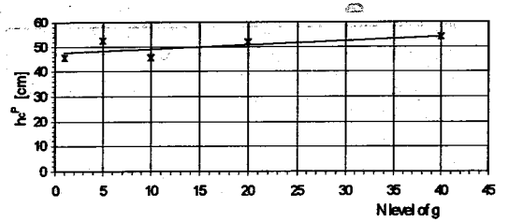

Figure 6. Final prototype capillary rise h_c^P versus Ng-level. (Bochum).

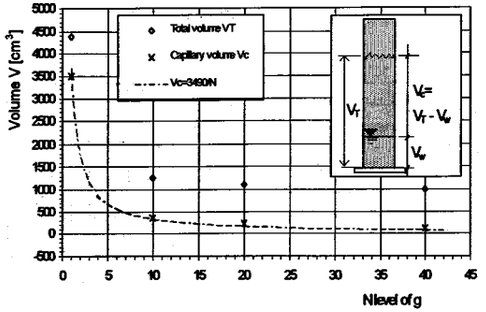

Figure 7. Model exchanged water volumes (V_T: total volume of water transferred into the sand sample, V_c: volume of capillary water).

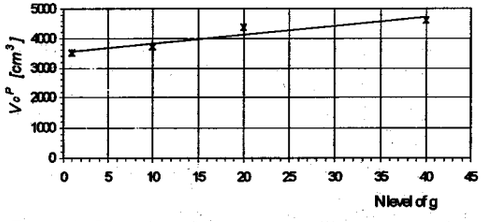

Figure 8. Linearity of prototype capillary water volume V_c^P versus Ng-level (Bochum).

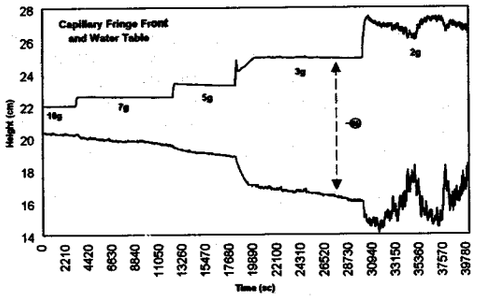

Figure 9. Capillary fringe front (top curve) and water table (bottom curve) versus time (Cardiff).

that has already been seen in Figure 6 derived from optical measurements.

6 CARDIFF TEST RESULTS

M. Davis, S. Burkhart

In this study of the scaling laws for capillary rise in a medium fine poorly graded sand, two different zones within the fringe are distinguished: one continuous zone for the liquid phase, where the sand is almost saturated, and a second discontinuous one with a saturation ratio less than 75%.

6.1 Results of the volumetric measurement

Figure 9 presents the capillary rise and the respective water table during the second dry to wet test at different g-levels. Δh_{CF} is the saturated capillary fringe above the fluctuating water table level and it has to be noted that the g-levels in the figure below are not the effective g-levels. These results are plotted from the information received from the tensiometer's and PPT's response.

On the graph a strong correlation between the two curves may be seen. A strange oscillation is also noted at 2g, with water being transferred alternatively between the reservoir and the column, with the fringe following the water table. Probably this happens due to the uncontrolled periodic acceleration level at this low value.

The scaling law for the rate of growth of this continuous zone was difficult to assess during these tests; but it could be seen a tendency for a faster growth as the g-level was decreasing. On the contrary, the rate of growth of the discontinuous part seems to be constant and independent of the g-field, revealing the existence of a suction mechanism in microscopic scale around the grains.

The question raised is the validity of a quasi-static description for suction phenomena far from equilibrium in a enhanced g-field.

6.2 Static scaling law for dry to wet tests

The 1/N scaling law for the capillary rise above the water table is taking in account only the continuous part and it is obtained by plotting the capillary rise against the g-level corrected for the non-uniformity of the acceleration field along the column. Provided that the final saturated capillary fringe is displayed against the corrected g-levels someone can get a fairly good agreement with the expected simple scaling law as it can be seen below (Figure 10). In this figure, TS and PPT are the data from suction (tensiometer) and pore pressure measurements and EXPECT are the results of the equation:

$$\Delta h_{cf} = 23,7/N \qquad (\Delta h_{cf} \text{ in cm}).$$

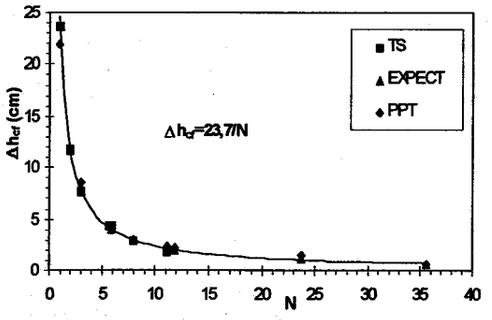

Figure 10. Scaling law obtained from dry to wet tests (Cardiff).

This figure shows a good consistency of the results obtained from the electrical instrumentation used during the tests (tensiometers and PPT's) with the results expected from the theoretical point of view concerning the saturated capillary rise.

A very important point concerning the above scaling law is that the characteristic pore size for the sand used during these tests is estimated as d=129μm. This pore size is slightly higher than the effective grain size d_{10}=100μm which was proposed to be used as the characteristic pore size.

Concerning the stress level, it doesn't seem to play any role on the scaling law, as we compared the final states from both tests, corresponding to a 1m sand column for the first dry to wet test and a 50 cm sand column for the second test.

7 DISCUSSION

D. König, A. Rezzoug

The Manchester experiments on fine HPF5 sand (d_{10}=0,05mm) show an agreement with time scaling:

$$t_c^P = t_c^M \cdot N^2 \qquad \text{(Figures 2 and 3).}$$

Unfortunately the duration of the tests at the lower g levels is perhaps to short to detect the true final height of capillary rise.

The final volume has been measured and approximately evaluated in the Cardiff and Bochum tests on Congleton sand (d_{10}=0,1*mm*) and on Normsand (d_{10}=0,12*mm*). The relationship:

$$h_c^P = h_c^M \cdot N$$

is well fitted by the tests results on Congleton sand. The result of tests on Bochum Normsand deviates slightly from this scaling relationship. This may be due to difficulties in the measurement of the small capillary rise for such soils at the higher g levels. But also the effect of the gravity on the shape of the menisci and on the capillary pressure as mentioned by Shubert 1982 (see §2.1.of this Chapter) may be relevant. This effect becomes more important for coarser soils.

An other possible reason could be the effect of stress level. However, for practical use of centrifuge modelling in sands with $d_{10} \leq 0,1mm$ it seems to be verified that capillary rise from dry to wet conditions is properly scaled by N.

The deviation in time scaling is more significant. The relationship $t_c^P = t_c^M \cdot N^2$ is not so clear from the results on Bochum sand shown in Figure 4. Some tests will be performed in Bochum on Congleton sand to verify this question.

Further study in the Working Group will be concentrated on drainage tests. Probes for measuring the water content profiles in the sand sample during the centrifuge model tests will be used. Such probes are described in § 2 of the Chapter II.

IV CENTRIFUGE RESEARCH ON THE TRANSPORT OF NAPL's

F.A. Weststrate, J.T. van der Poel, Delft Geotechnics, NL

As a part of the NECER programme, research is being executed on the possibility of performing centrifuge model tests on NAPL transport problems and determination of scale relations for NAPL transport. The scaling of the phenomena of entry pressure, NAPL flow and residual saturation are studied. The research will continue until September 2000. In this paper preliminary results are presented. The tests concern the flow of DNAPL's through water-saturated sand and LNAPL's through partially saturated sand. The tests, discussed in this paper, have been performed by Delft Geotechnics, Delft University of Technology, City University in London and University of Cambridge. The results are encouraging, but more tests and analyses need to be done.

1 GENERAL INTRODUCTION

Dense non-aqueous phase liquids (DNAPL's), like perchloroethylene (PCE) and trichloroethylene (TCE), are widely used as degreasers, solvents and in the dry cleaning. Due to their physical and chemical characteristics PCE and TCE expose serious environmental hazards. As these chemicals have a density of about 1.5 times the density of water and are hardly soluble in water, these liquids have a tendency to sink into the soil system as pure liquids. Once they reached a barrier like the bottom of an

aquifer, they are a continuous source of groundwater contamination.

The vertical transport velocities of these DNAPL's are of main importance with respect to the contaminant source area to be expected and consequently to the possible risks, sanitation possibilities and costs. Experimental and theoretical research on the transport behaviour of DNAPL's show that the physical/chemical characteristics as well as soil heterogeneities strongly influence the transport in saturated and unsaturated systems. Almost all of this research is restricted to 1g experiments in thin slit models as well as in natural systems.

As DNAPL's have a density higher than water the transport behaviour in soil materials of these chemicals could be studied by centrifuge experiments. This means that smaller models, compared to 1g models, can be used which can be scaled up to 1g conditions and that, experimental time can be reduced. Besides that experiments can be performed under the same stress levels as in reality. If using large centrifuge facilities even more than one experiment can be performed during one flight.

Light non-aqueous phase liquids (LNAPL's), like motor oil, differ from the DNAPL's by its density. They have densities smaller than the density of water. It means that they will float on the top of the capillary fringe. They also expose environmental hazards. Modelling the transport of LNAPL's in a geotechnical centrifuge is only possible for partial or unsaturated soil systems, due to the low densities of the LNAPL's.

The objective of this part of the NECER programme is to investigate the possibilities of modelling NAPL transport in a centrifuge and to determine scale relations. In the NECER programme both NAPL's are studied and two basic centrifuge test types are performed: The first type of tests are the 1-dimensional column tests, for modelling the entry pressure, flow characteristics and the residual fractions of DNAPL's for different soil systems. The second test type is the 2-dimensional centrifuge test, using a strongbox, for modelling the propagation of a NAPL plume in time and the residual fractions after propagation.

2 CENTRIFUGE RESEARCH ON THE TRANSPORT OF DNAPL'S

A series of preliminary tests have been performed in a column and a table centrifuge to study the flow behaviour of the DNAPL PER in water saturated sand. The objective was to obtain an impression of processes, velocities of DNAPL flow and residual saturation. A case of a non-wetting fluid displacing a wetting fluid vertically downward through homogeneous and isotropic porous media was considered. The tests have served as a basis for designing a set-up for tests in the large geocentrifuge.

2.1 DNAPL transport at 1g : preliminary tests

O. Oung.

All 1g tests have been performed in a perspex column of 140 mm diameter and a sand sample of 100 mm height. The first aim was to prepare reproducible Baskarp sand samples of 34% porosity and 95% relative density. The properties of the Baskarp sand are given in Table 1.

In this table γ_s is the specific weight of the grains, n_{min} and n_{max} the minimum and maximum porosity, d_{50} the average grain size and d_{60}/d_{10} the uniformity index of the sand. The PER has a density of 1623 kg/m^3, a kinematic viscosity of $0.6*10^{-6}$ m^2/s. The surface tension between PER and water is 47.5mN/m.

Table 1. Properties of Baskarp sand.

γ_s (kN/m^3)	n_{min} (%)	n_{max} (%)	d_{50} (mm)	d_{60}/d_{10} (-)
26.0	34.2	47.0	0.14	1.7

Test results

The tests have been performed by applying a small hydraulic gradient over the sample. The obtained permeability values, determined by measuring the outflow of water, are shown in Table 2.

A second series of measurements was carried out allowing the other fluid to infiltrate. When either the PER content or the water content reached its maximum, the effective permeability was then measured. The results are shown in Table 2. The effective permeability of a sample containing a residual fraction of water is ~25% lower than the three other values. As PER is the non-wetting phase, it is likely that its flow should be slowed down by the presence of the irreducible fraction of water.

The second aim of the work was to study the infiltration process of PER into a water-saturated sample. A value of 170 ± 10 mm of PER was found for the entry head which is in good agreement with the calculated one.

The average front was sharp despite observation of a few fingers formation of 1-2 cm length at edges. After excavation of the sample no preferential path

Table 2. Permeability determination.

Sample	(Effective*) Permeability (m/s)
Water-saturated	5.7 E-5 (± 10 %)
Water + residual fraction of PER	5.1 E-5 (± 10 %)
PER-saturated	6.7 E-5 (± 8 %)
PER + residual fraction of water	1.5 E-5 (± 10 %)

*After infiltration of the other fluid

was observed. The outflow of PER was observed only when the front reached the end of the sample. As the whole infiltration process was rather slow, it indicates that only a minimum of fingering formation into the samples has occurred.

Another series of experiments showed the influence of the pressure head on creating a sharp front. By increasing the head step by step (~ 2 cm), the PER could only invade the corresponding distribution of the pore volume.

The higher the pressure, the more pore space is filled. This shows that the PER content depends on the hydraulic gradient. As a sharp front formation condition was to be generated, a high head was set at start, so that as the front went further it filled the maximum of the pore volume. Figure 1 shows the sample. The dark coloured part indicates the position of the DNAPL.

The third aim of the study was to determine the residual saturation of DNAPL. When the sample was saturated with DNAPL, water was allowed to flush through it. A residual saturation was then reached. Slices of the sample were taken every 1cm and analysed by spectrophotometry. The residual saturation range found was 2-5% of the pore volume. These results are in good agreement with values given in the literature.

Discussion and conclusion

According to the phase diagram of displacement regime (Lenormand, 1985), the experiments should belong to the transitional phase. Since the gravitational component was not taken into account for this diagram, conditions to obtain a sharp front of the DNAPL flow has to be determined.

The preliminary tests done at 1g gave valuable information on the experimental conditions to create a sharp front. Respectively, if the gradient is high enough then the front tends to be sharp, otherwise preferential paths are firstly fulfilled. One should notice that the samples had a high degree of compaction and an unavoidable layering of fines at

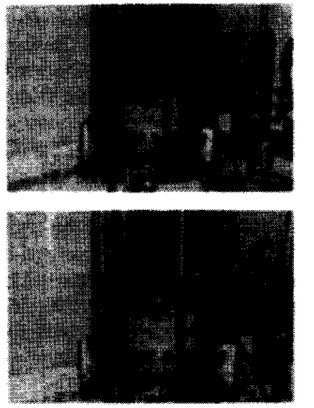

Figure 1. Flow front observation

compaction limits, which might enhance the sharpness of the front or limit fingering process and for what the phase diagram doesn't take into account. The fact that the PER content depends on the differential pressure indicates a scaling factor for this parameter.

2.2 1-Dimensional centrifuge experiments

F.A. Weststrate & J.T. van der Poel

Three test series have been performed at different g-levels. The running time has also been varied in the test series. After the tests the DNAPL content over the height has been determined by slicing the sample.

Materials and methods

The tests have been performed in the table centrifuge. In this small centrifuge, two centrifuge cups are used and tested simultaneously. In the cups a compacted sand sample has been placed with a height of 60 mm. On the bottom of the cups a brass filter has been used to allow drainage of water and PER from the cup to the centrifuge container. The cups are placed and fixed into the containers of the small centrifuge. These containers are filled with water to the same level as inside the cups. The tests have therefore been performed at an almost constant water table. The water table in the 1g situation was 10 mm above the sand surface.

The cups have a diameter of 67 mm. The radius from the centre of rotation to the top of the sand model is 130 mm and 190 mm to the bottom of the sand sample. This means that the g-level will vary significantly over the model height. Also, due to the relatively large diameter compared to the radius,

curvature of the water table plays a significant role.

The sand that has been used was the Baskarp sand. The properties of the sand are given in Table 1. The sand has been compacted by wet tamping of thin layers to a relative density of 88%.

Test procedure

The centrifuge was first spun up to the required level. Then PER was injected by means of a peristaltic pump. The PER was injected below the water table. Before injection the PER was coloured with the Sudan red dye. The centrifuge was then spun for several minutes to hours.

After the test, water was drained from the bottom of the sample to generate capillary underpressures. Then the sand was excavated in layers with a thickness of 5 mm by means of a slicer. The PER concentration at the end of the test was determined by measuring the amount of dye per slice. First, the dye was separated from the sand. Then the dye concentration was measured by spectrophotometry. The amount of dye per slice was related to the dye concentration dissolved in the PER before the test to determine the residual concentrations.

Results

The performed centrifuge tests using the small centrifuge and their initial conditions are shown in Table 3.

The results of the test runs at 40 g are shown in Figure 2. In this figure the residual DNAPL fraction, (volume of DNAPL/pore volume sample) is plotted against depth for different flight times. The soil columns tested at 40g were sliced in parts of 0.5 cm thickness for analysing the residual DNAPL content. The soil column tested at 80g was analysed as a whole and showed a residual fraction of 4%. The test at 26g showed no breakthrough of DNAPL, indicating that the PER pressure was lower than the entry pressure.

The result of the 26g test is in agreement with the calculated entry head, compared to the actual entry head for the performed experiments (seeTable 4).

Table 3. Test run conditions

Run	Gravity level (g)	DNAPL injected (ml)	Injection time (min.)	Flight time (hrs)
1	26	12	1.5	0.5-2-4.7
2	40	30	1.5	0.25-0.5-2
3	80	15	10	0.5

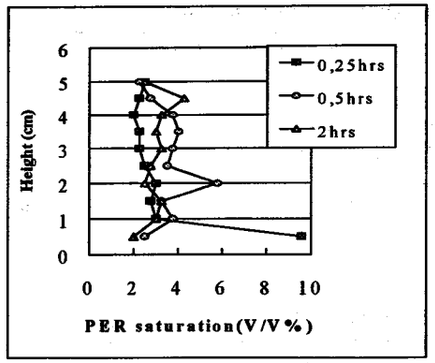

Figure 2. PER saturation at 40g

Table 4. Entry heads according to Pankow and Cherry 1996.

Gravity level (g)	calculated entry head (mm)*	actual entry head (mm)
1g	180	-
26g	6.9	>3.4[1]
40g	4.5	8.5
80g	2.3	4.2

[1]No entry occurred

Due to the curvature of the meniscus during the tests, the DNAPL height at the outer part of the column will rise with 1.4 mm compared to the original surface level. This correction is not included in Table 4. The curved meniscus also means that if the head will exceed the entry head, it will happen at the outer part of the column. This is also the reason that after the 80g and 40g experiments some DNAPL was left on top of the column. Analysing the residual DNAPL content of the first two top slices showed an increased DNAPL content, due to the presence of the DNAPL that was left on top. For this reason the data of the first two slices (from 6cm to 5cm) are not shown in Figure 2.

The 40g test has also been simulated by the 3-phase model SWANFLOW. The relative permeabilities have been estimated on the basis of the fractions of PER and water, the viscosity of the fluids and densities. The results of the calculated residual fractions in depth and in time are presented in Figure 3.

Discussion and conclusions

Although the results of the preliminary tests at 40g show some scatter with depth, possibly due to the sampling method, it can be concluded that 1-

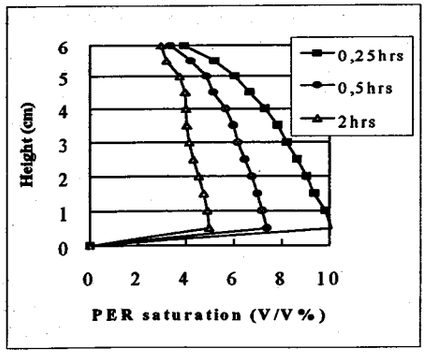

Figure 3. Modelled PER fractions.

dimensional centrifuge tests may offer a good and fast method for the research on DNAPL transport. From the figures it can be seen that the modelled fractions (Figure 3) are 2 to 3 times higher than the experimental results (Figure 2).

The difference is probably caused by the fact that in the experiments in the small centrifuge the DNAPL is not flown through the total volume of the sample due to the curvature of the water table and the horizontal component of the acceleration near the edges of the cup. Corrections for the flown through part of the volume can be made and are in between 75% at the top to 25% at the bottom. Another aspect is the increase of g-level with depth (35g at the top, 45g at the bottom), thereby increasing the hydraulic conductivity with depth. The 3-phase model can not model this variation in g-level over the column height.

3 TWO-D MODELLING OF DNAPL TRANSPORT IN HOMOGENEOUS SATURATED SOILS

S.M. Spiessl, R.N. Taylor

Geotechnical centrifuge modelling may be used to study flow of immiscible fluids in porous media (Illangasekare et al., 1991) provided scaling laws are not violated. Petersen and Cooke (1994) suggested some potential problems with scaling relations for finger length, critical wavelength and growth rate of an advancing pollutant front. Thus the validity of centrifuge modelling for such transport problems still requires investigation, and the work described is a preliminary study of two dimensional DNAPL flow through homogeneous and saturated soils using the centrifuge facility at City University.

3.1 Model tests

The tests were conducted in a purpose-built strong box 398mm wide by 349mm high, and with a breadth of only 28mm, which was made deliberately small for the plane strain model testing. The soil material consisted of spherical glass beads with particle size in the range 100-200 μm. A drainage base was available as a collection reservoir for the DNAPL PER after it had flowed through the model. Rimmer et al (1996) showed that the wetting properties of a fluid have a major influence on the flow along a boundary. Wilson et al (1989) suggested that it was advisable to use a hydrophilic boundary (e.g. glass) for hydrophilic media (glass beads) to prevent oil-preferential wetting of the boundary, since perspex is hydrophobic, as is PER. As a consequence, the centrifuge strong box was lined with glass plates, which were roughened by sandblasting to minimise preferential sidewall flow.

PER was injected into the soil below the ground surface to avoid problems of surface flooding with possible obscuring of flow mechanisms through the soil. The injection point was a narrow (4 mm wide) slot at the centre of the model and which penetrated 38mm into the ground. The injection system was designed so that potential hydraulic fracture by the in-flowing PER was avoided.

3.2 Preliminary results and discussion

Figure 4 shows typical DNAPL plume development with time recorded by an on-board CCTV camera during a 5g test.

The plume initially spreads fairly uniformly from the injection point, and although the edge of the plume has some irregularities there is no evidence of fingering indicating unstable flow. It is planned that image analysis software will be used to interpret the differences between images and a reference image at the start of the test, and from this the edge of the plume will be determined and its position measured. Thus the area of the plume, and hence the volume

a) 88 sec. after DNAPL injection | b) 236 sec. after DNAPL injection | c) 604 sec. after DNAPL injection

Figure 4. Digital images showing DNAPL plume development in Run 2 with time.

flow of PER (for plane strain conditions) can be estimated. At this stage, an approximate manual method has been used, and the results for the different runs, identified in Table, are compared in Figure 5. Here, the data have been converted to equivalent prototype time by multiplying both plume area and model time by N^2 where N is the centrifuge acceleration.

Though there is some similarity between the tests, there are some unexpected differences. The two runs with 10g (Runs 4 and 5) were different by a factor of about 2. Run 7 (at 8g) was similar to Runs 2, 3 and 7 (at 5g). Explanation of this behaviour is difficult and more data are needed to understand the processes involved. However, part of the explanation may be linked to different saturation times and void ratios, given in Table 5.

Although the dry soil had CO_2 injected to assist in later saturation, nevertheless the saturation times used may still leave some trapped air (Christiansen, 1944; Faybishenko, 1995) which would affect adversely the hydraulic conductivity of the samples. Also, the hydraulic conductivity changes with soil packing, or void ratio. Clearly these factors cannot explain all the differences between the tests, and more needs to be done to investigate the likely hydraulic conductivity of the individual models.

Table 5. Initial conditions of the six runs.

Run	Void ratio	Time for saturation from below (hrs)	Gravity
2	0.55	13.50	5
3	0.92*	20.80	5
4	0.60	21.28	10
5	0.59	38.60	10
6	0.59	37.47	5
7	0.50	62.13	8

* uncertainty in value

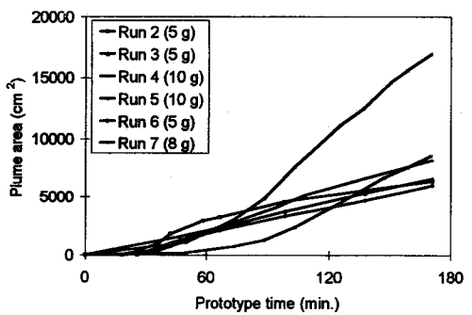

Figure 5. Development of plume area with time for Runs 2 through 7.

Another potential explanation of differences between tests is the possible deviation from plane strain flow. Figure 6 shows two views of Run 2 after the test during excavation of the soil sample. The upper picture is a view from the top of the box after the upper 37mm of the sample had been removed. The dark stain in the central part of the sample indicates the plume width. The lower picture shows a view through the front window taken at the same time and this view suggests a wider plume at the excavated surface. The implication is one of preferential boundary flow, but it is not possible to say whether or not this occurred during the course of the centrifuge test. It is an issue requiring further investigation, possibly by using discrete transducers buried at the mid-plane of the soil sample.

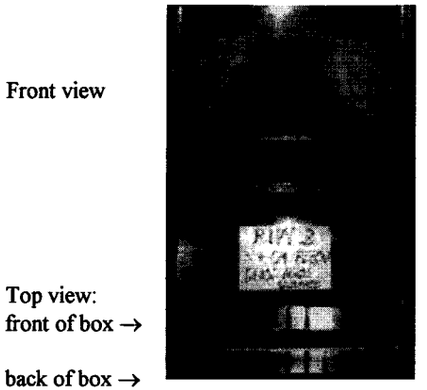

Figure 6. Example of preferential boundary flow view from front window-side of model, and corresponding view from top of model excavated to 3.7 cm below surface.

Figure 7: Photograph with the final pattern of the DNAPL plume at a similar 1-g experiment in an inclined layered saturated system (from Coumoulos et al, 1998).

3.3 Summary

A series of model tests investigating the potential use of a geotechnical centrifuge for studying problems of DNAPL flow has been undertaken. The problems of preferential flow along a boundary have been minimised by using a model container lined with roughened glass plates. The initial results are encouraging, but more work is needed to be able to measure with greater precision the size of the PER flow plume as it develops, and to relate this to the centrifuge test acceleration and the hydraulic properties of the soil.

4 DNAPL EXPERIMENT IN AN INCLINED LAYERED SATURATED SYSTEM

H. Coumoulos & K. Soga

A DNAPL migration experiment was performed in the Geotechnical Centrifuge Centre at Cambridge University. The aim was to examine the effect of the increased gravity field in the migration pattern and speed in a two layer system with an inclined interface.

4.1 Experimental set-up

The porous medium used was uniform spherical glass beads of two sizes: coarse with D_{10}=0.466 mm and fine with D_{10}=0.222 mm. The model was poured dry from a hopper via a flexible tube. It was saturated from the bottom, first with CO_2 and then with de-aired water. The centrifuge package is shown in Figure 9 and Figure 10. Its width is 150mm.

The DNAPL used was the 3M perfluorocarbon fluid HFE7100, which may be used as a safe alternative to the commonly used DNAPLs, such as TCE, PCE and other toxic chlorinated solvents (Miller, 1996). To enable visual observation, the fluid was dyed blue with the 3M dye FC3275. The HFE7100 has a density of 1500 kg/m^3, viscosity of 0.61 mPa.s and surface tension of 13.6 mN/m.

The fluid was injected on a horizontal line spanning the width of the model, at 100 mm depth. The source was perpendicular to the front window, so it represents a point source, in 2 dimensions. The injection was of the falling head type. It was initiated in-flight by the opening of a pneumatic valve placed on the top surface of the model. The rate of injection was monitored with Pore Pressure Transducers (PPT) at the base of the header tanks.

The fluid injection caused water to drain from the bottom of the model to a collector tank. The rate of outflow was also monitored by a PPT at the bottom of the tank. The DNAPL migration was monitored by a colour video camera mounted on a frame on the front of the package

4.2 Results

A sequence of pictures showing the progress of the DNAPL plume with time is presented in Figure 8. Figure 7 shows similar 1-g experiments (Coumoulos et al., 1998). Comparing Figure 8 and Figure 7, the effect of increased gravity field on DNAPL migration patterns is demonstrated.

5 CENTRIFUGE MODELLING OF LNAPL TRANSPORT IN PARTIALLY SATURATED SOILS

G.M. Esposito & H.G.B. Allersma

LNAPL transport in partially saturated soils can be physically modelled in a geotechnical centrifuge (Knight and Mitchell, 1996). Two-dimensional tests at 30g have been performed in the geotechnical centrifuge at the University of Delft. In order to provide detailed information, the phenomena were observed in flight by using video cameras and image processing (Allersma, 1997). Thanks to this observation technique, a good understanding of the non-aqueous phase liquid movement in the subsurface can be obtained.

5.1 Kinematics of LNAPL flow

The LNAPL phase was simulated by oil having a density of 950 kg/m^3 and a viscosity of 0.142 Pa.sec. The observation of 2-dimension LNAPL flow through an unsaturated sand (D_{50} = 0.2 mm, water content w = 5%) provided information about the flow domain, the velocity field, and the relationship porosity-kinematics flow characteristics. Figure 11 shows the variation with time of the flow domain during a test on Silver Sand. The shapes and areas of the plumes were measured and correlated to the variation of the LNAPL head with time.

Time indicated in Figure 11 refers to the model time. During the experiments, the movement of certain points of the LNAPL plume were recorded and their position in time was made to fit to theoretical curves. For example (Figure 12), the position of the most advanced point of the front of the LNAPL in time was:

$$E_f = C_1 t^{\frac{1}{2}} + C_2 t$$

where C_1, and C_2 depend on the soil density, and t is time.

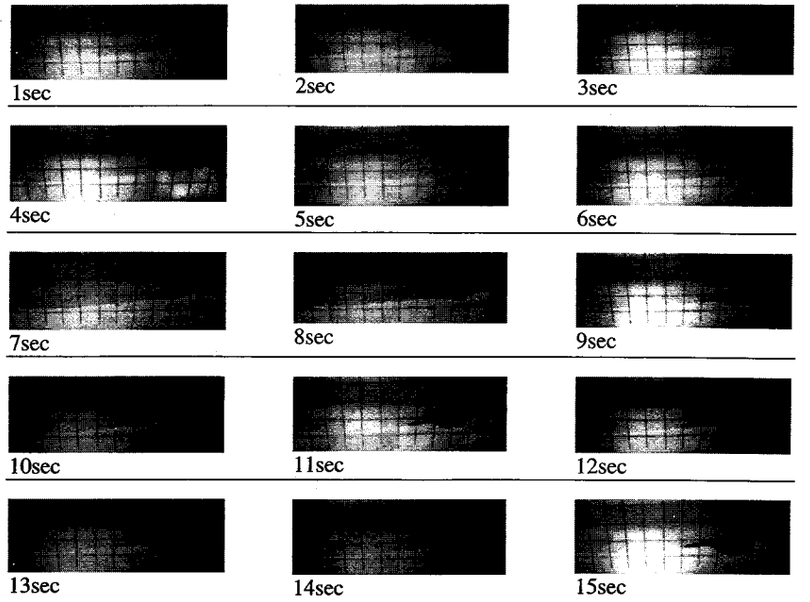

Figure 8. Photographs with location of the DNAPL plume at different times

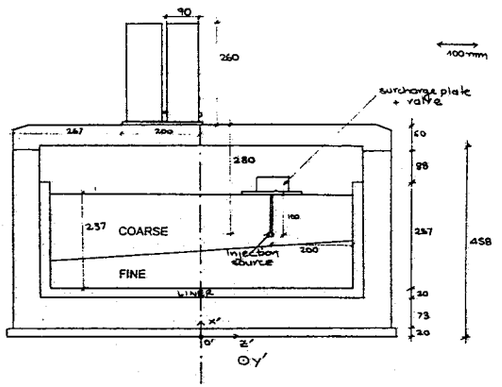

Figure 9. View of the centrifuge package from the front

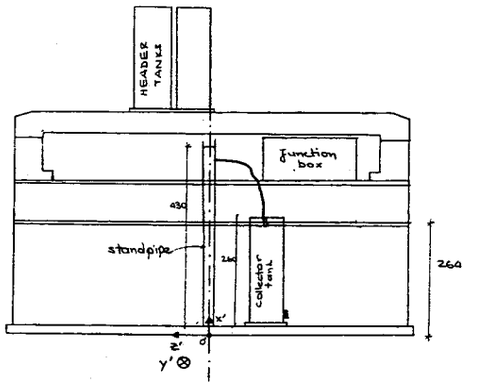

Figure 10. View of the centrifuge package from the back

At any instant of time, the actual volume occupied by the LNAPL in the flow domain was correlated to the volume discharged from the tank. Figure 13 shows that the available pore volume in the flow domain is completely LNAPL-saturated during the LNAPL

5.2 Measurements of saturation

Measurements of LNAPL content were carried out by means of the image processing technique. The technique consisted of measuring the grey levels of the images of the plumes taken during the progress of the test.

The values of light intensity obtained were correlated to gravimetric measurements of LNAPL content carried out at the end of the tests. Figure 14

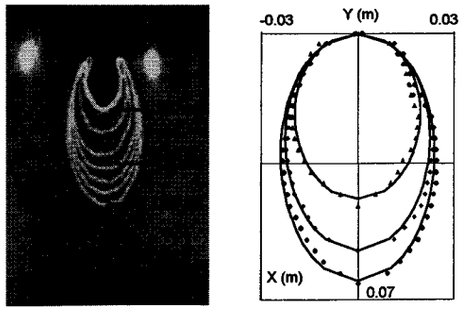

Figure 11. Picture (a) and fit (b) of the plumes in time (120, 510 and 1320 sec.).

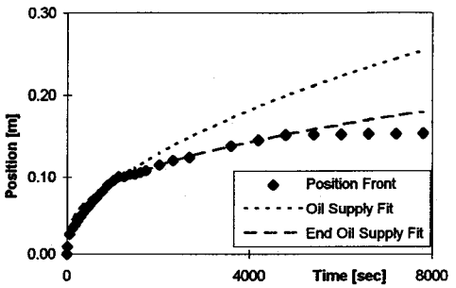

Figure 12. Position of the LNAPL front in time discharge.

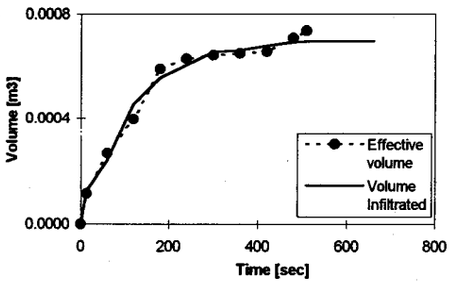

Figure 13. LNAPL and plume volume during the discharge.

shows an example of variation of the LNAPL concentration in time along the axis of the plume. Finally, the scaling laws governing the dynamics of the centrifuge was studied too. Figure 15 shows the relation between residual saturation and g level expressed as inverse of the Bond number.

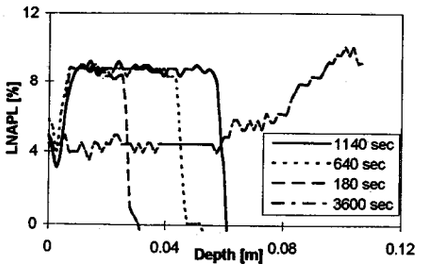

Figure 14. LNAPL concentration in the plume.

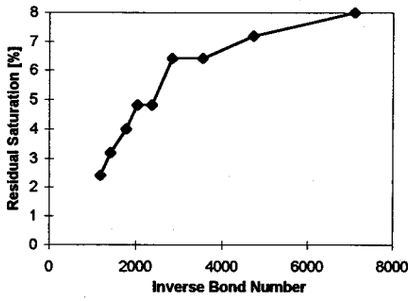

Figure 15. Residual saturation vs Bond number.

ACKNOWLEDGMENTS

This research effort is part of the NECER programme (Network of European Centrifuges for Environmental Geotechnic Research). The project is supported by the European Community under contract FMRX-CT96-0030 in the Training and Mobility of Researchers Programme (DG XII Science, Research and Development). The financial assistance of the Commission is sincerely appreciated.

MISCELLANEOUS

More information is available on the NECER web site: http://www.lcpc.fr/~necer/necerwww.htm.

REFERENCES

Allersma, H.G.B. 1990. One line measurement of soil deformation in centrifuge tests by image processing, *9th Int. Conf. On Exp. Mechanics*, 4:1739-1748.

Allersma, H.G.B. 1997. Using imaging technologies in experimental geotechnics. *Proceedings of the 2nd International Conference Imaging Technologies*. (eds. J.D. Frost, S. McNeil), ASCE: 1-9.

Arulanandn, K. and Kutter, B.L. 1988. Centrifuge modelling of transport processes for pollutants in soils. *J. of Geotech. Ing.*, Vol.114, n°2.

Arulanandan, K., Thompson, P.Y., Kutter, B.L., Meegoda, N.J., Muraleethan, K.K., Yogachandran, C. 1988. Centrifuge modelling of tranport processes for pollutants in soil. *J. Geot. Eng. ASCE*, Vol.114 (2): 185-205.

Coumoulos, H, Kechavarzi, C, Soga, K. and Illangasekare, T. 1998. 2D NAPL experiments using the CU γ-ray syste. *CUED Internal report.*

Cooke, A.B., Mitchell, R.J. 1991a. Physical modelling of a dissolved contaminant in partially saturated soils. *Canadian Geot. J.* 28: 829-833.

Cooke, A.B., & Mitchell, R.J. 1991b. Evaluation of contaminant transport in partially saturated soils. *Centrifuge 91.* Boulder, Ko H.Y.(ed), Balkema.

Cooke, A.B. 1994. Determination of soil hydraulic properties: *Centrifuge 94,* Leung, lee & Tan (eds). Balkema, Rotterdam.

Corte, J.F. and Garnier, J. 1992. Measuring techniques in centrifuge model tests. *Prof. Jessberger's Volume,* Balkema : 29-42.

Christiansen, J.E. 1944. Effect of entrapped air upon the permeability of soils. *Soil Science*, 58: 355-365.

Culligan-Hensley, P.J. & Savvidou, C. 1995. Environmental geomechanics and transport. In R.N. Taylor, *Geotechnical centrifuge technology*: 196-263. Balkema.

Culligan, P.J., Barry, D.A., Parlange, J.Y. 1997. Scaling unstable infiltration in the vardose zone. *Canadian Geot. J.* 34: 466-470.

Dupas, A., Cottineau, L.M., Garnier, J. 1995. Moisture content measurement in centrifuge models. *1st Int. Conf. On Unsaturated Soils,* Paris: 1-5.

Faybishenko, B.A. 1995. Hydraulic behavior of quasi-saturated soils in the presence of entrapped air: Laboratory experiments. *Water Resources Research,* 31(10): 2421-2435.

Goodings, D.J. 1984. Relationships for modelling water effects in geotechnical centrifuge models. *Proc. Of Int. Symp.on the application of centrifuge modelling to geotechnical design,* Manchester 1984. Graig, Wlt (eds).

Goforth, G.F., Townsend F.C., & Bloomquist D. 1991. Saturated and unsaturated fluid flow in a centrifuge. *Centrifuge 91.* Boulder, Clorado, Ko H.Y.(ed), Balkema.

Hensley, P.J. 1989. Accelerated physical modelling of transport processes in soil, *PhD Thesis,* University of Cambridge.

Illangasekare, T.H., D. Znidarcic, M. Al-Sheridda and D.D. Reible. 1991. Multiphase flow in porous media. *Centrifuge 91,* Boulder, Ko (ed). Balkema.

Knight, M.A., Mitchell,R.J. 1996. Modelling of light nonaqueous phase liquid (LNAPL) releas into unsaturated sand. *Canadian Geotechnical Journal,* 33 (4): 913-925.

Knight, M.A. & Mitchell, R.J. 1996. A similitude and dimensional design guide for centrifuge modelling of multiphase contaminant transport. *Envir. Geotech.* Kamon (ed.) Balkema: 245-250.

Knight, M.A., & Mitchell, R.J. 1995. Centrifuge modeling of multiphase flow in the vadose zone: *Geonvironmental 2000. ASCE, New York. Geotecnical special Publication,* 46. Y.B. Acar, D.E. Daniel, Eds.

Lenormand, R. 1985. *C.R. Acad. Sci. Ser.2.* 310, 247-250,1985.

Li, L., Barry, D.A., Stone, K.J.L. 1994. Centrifugal modelling of nonsorbing, nonequilibrium solute transport in locally inhomogeneous soil. . *Canadian Geot. J.* 31: 471-477.

Miller, C. 1997. Immiscible fluid behavior in layered porous media: examples of accessibility and hysterisis. *MSc Thesis* Colorado State University.

Mitchell R.J., and Cooke B. 1991. An apparatus for in-flight constant head monitoring. *Centrifuge 91,* Boulder, Ko (ed.). Balkema.

Mitchell, R.J. 1994. Centrifuge techniques for testing clay liner samples. *Canadian Geot. J.* 31: 577-583.

Mitchell, R.J. 1994. Matrix suction and diffusive transport in centrifuge medels. *Can. Geotech. J.* 31. 357-363.

Mitchell, R.J., and Stratton, B.C. 1994. LNAPL penetration into porous media. *Centrifuge 94,* Singapore, Leung, Lee & Tan (eds). Balkema.

Mitcheson B. 1997. Geocentriguge modelling of capillary phenomena in unsaturated soils. *M.Sc. dissertation,* University of Manchester.

Padday, J.F. 1969. Theory of surface tension. Part I, II & III. *In: E., Matijevic: Surface and Colloid science, Wiley-Interscience.*

Pankov, J.F. and Cherry, J.A. 1996. Dense Chlorinated Solvents and other DNAPL's in Groundwater, *Waterloo Press,* LCCCN: 95-61690

Penn, M., Savvidou, C., Hellawell, E.E. 1996. Centrifuge modelling of the removal of heavy metal polluttants using electrokinetics. *Envir. Geotech.* Kamon (ed.) Balkema: 1055-1060.

Petersen, S.E., Cooke, B. 1994. Scaling concerns for immiscible multiphase flow in porous media. *Centrifuge 94.* Singapore, Balkema: 387-392.

Ratnam, S., Culligan-Hensley, P.J., Germaine, J.T. 1996. The behaviour of light, nonaqueous liquids under hydraulic flushing. *Environmental Geotechnics,* Kamon (ed), Balkema.

Rimmer, A., Parlange, J.-Y., Steenhuis, T.S., Darnault, C. and Condit, W. 1996. Wetting and nonwetting fluid displacements in porous media. *Transport in Porous Media,* 25: 205-215.

Schubert, H. 1982. Kapillarotät in porösen Feststoffsystemen. *Springer Verlanger,* Berlin, HEIDELBERG; New York.

Sills, B., & Mitchell, R.J. 1995. A new method for studying diffusion in unsaturated soil. *Geoenvironment 2000,* ASCE Geotechnical Special Publication, 46, Y.B. Acar, D.E. Daniel (eds), ASCE New York.

Taylor, R.N., Robson, S., Grant, R.J. and Kuwano, J. 1998. An image analysis system for determining plane and 3-D displacements in soil models. *Centrifuge 98,* Tokyo, Balkema.

Treadaway, A.C.J, Lynch, R.J. and Bolton, M.D. 1997 Pollution transport studies using an in-situ fibre-optic photometric sensor. *Geoenvironmental Engin. Yong & Thomas (ed),* London: 151-160.

Treadaway, A.C.J, Lynch, R.J., Bolton, M.D and Barker, H. 1998. Pollutant tracking with in-situ fibre-optic photometric sensors in a geotechnical centrifuge. *Proc. 3rd Int. Cong. on Environmental Geotechnics,* Lisbon.

Van Geel, P.J. and Sykes, J.F. 1994. Laboratory and model simulations of a NAPL spill in a variably-saturated sand, 1 : Laboratory experiment and image analysis techniques. *J. Contam. Hydrol.* 17 : 1-25.

Villar, H.P. 1993. The study of the movement of radioactive releases in soils using centrifuge modelling and radiotracer techniques. *PhD Thesis,* University of Manchester.

Villard, H.P., Merrifield, C.M., Craig, W.H. 1994. Experimental aspects of modelling of migration phenomena. *Centrifuge 94.* Singapore, Balkema: 363-368.

Wilson, J.L., S.H. Conrad, W. R. Mason, W. Peplinski, and E. Hagan, 1989. Laboratory investigation of residual liquid organics from spills, leaks, and the disposal of hazardous wastes in groundwater. *EPA/600/6-90/004.*

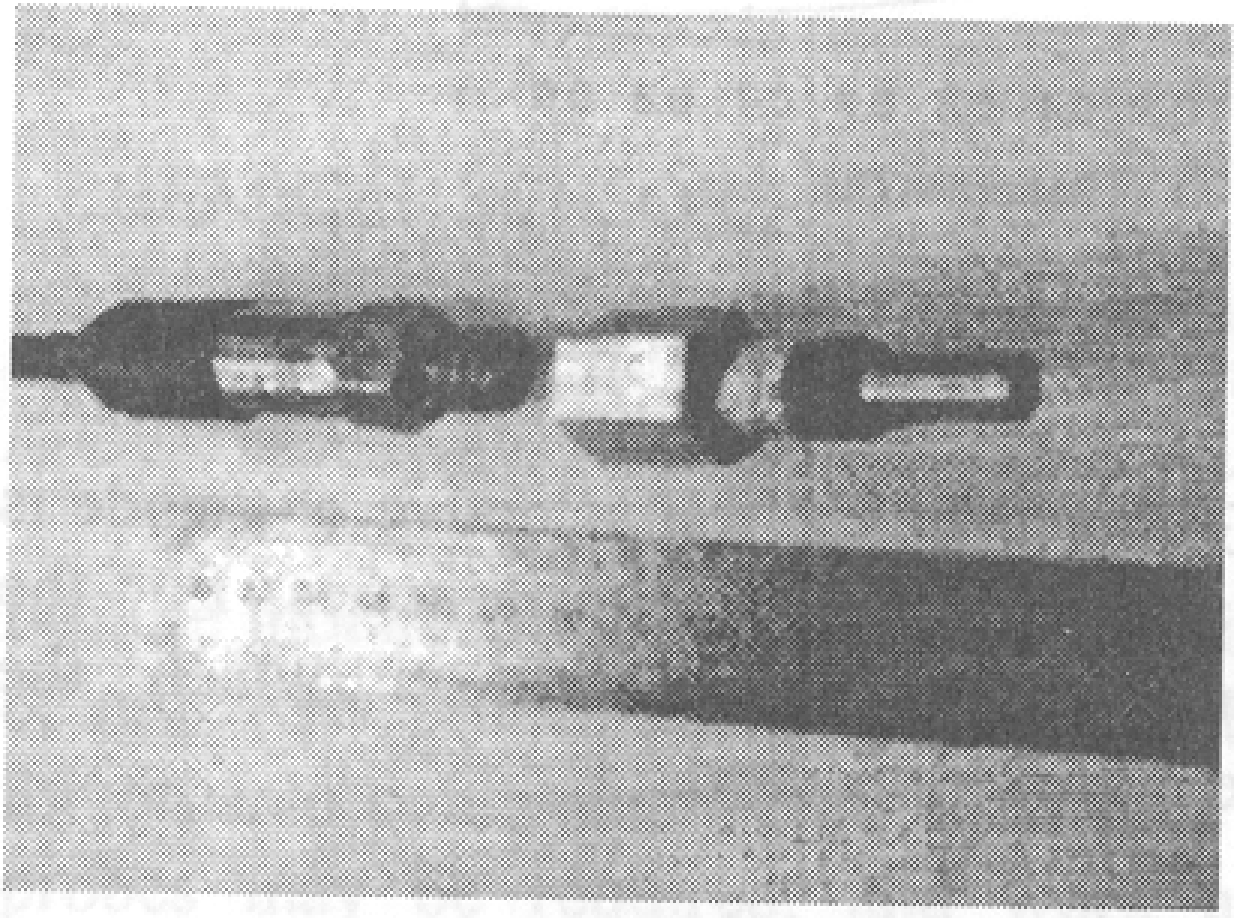

Figure 6a. NAPL and water tensiometer.

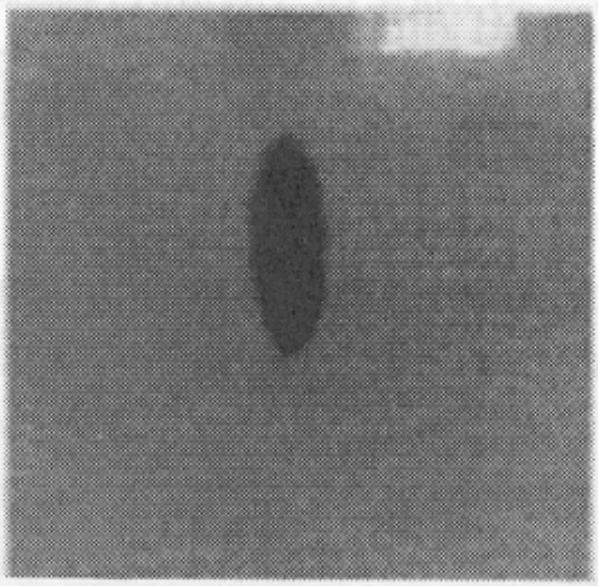

(a)

(b)

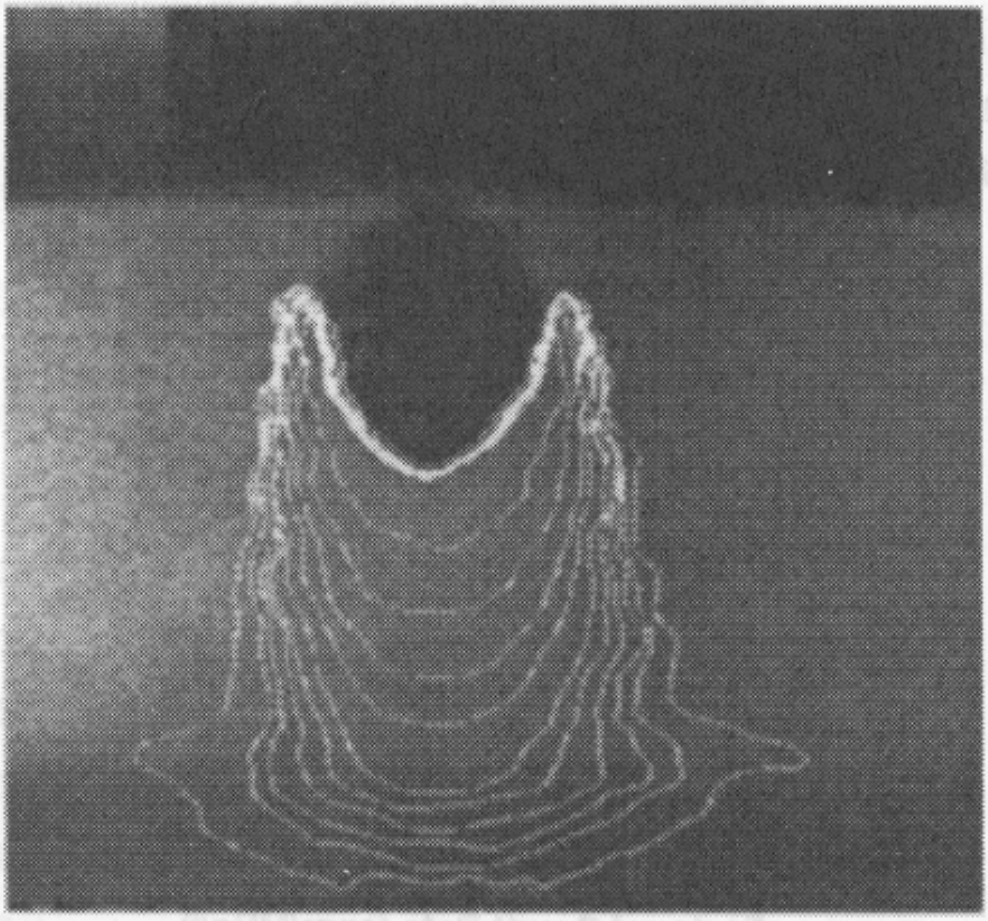

(c)

Figure 10 (a) Subtraction, (b) Threshold, (c) Contour.

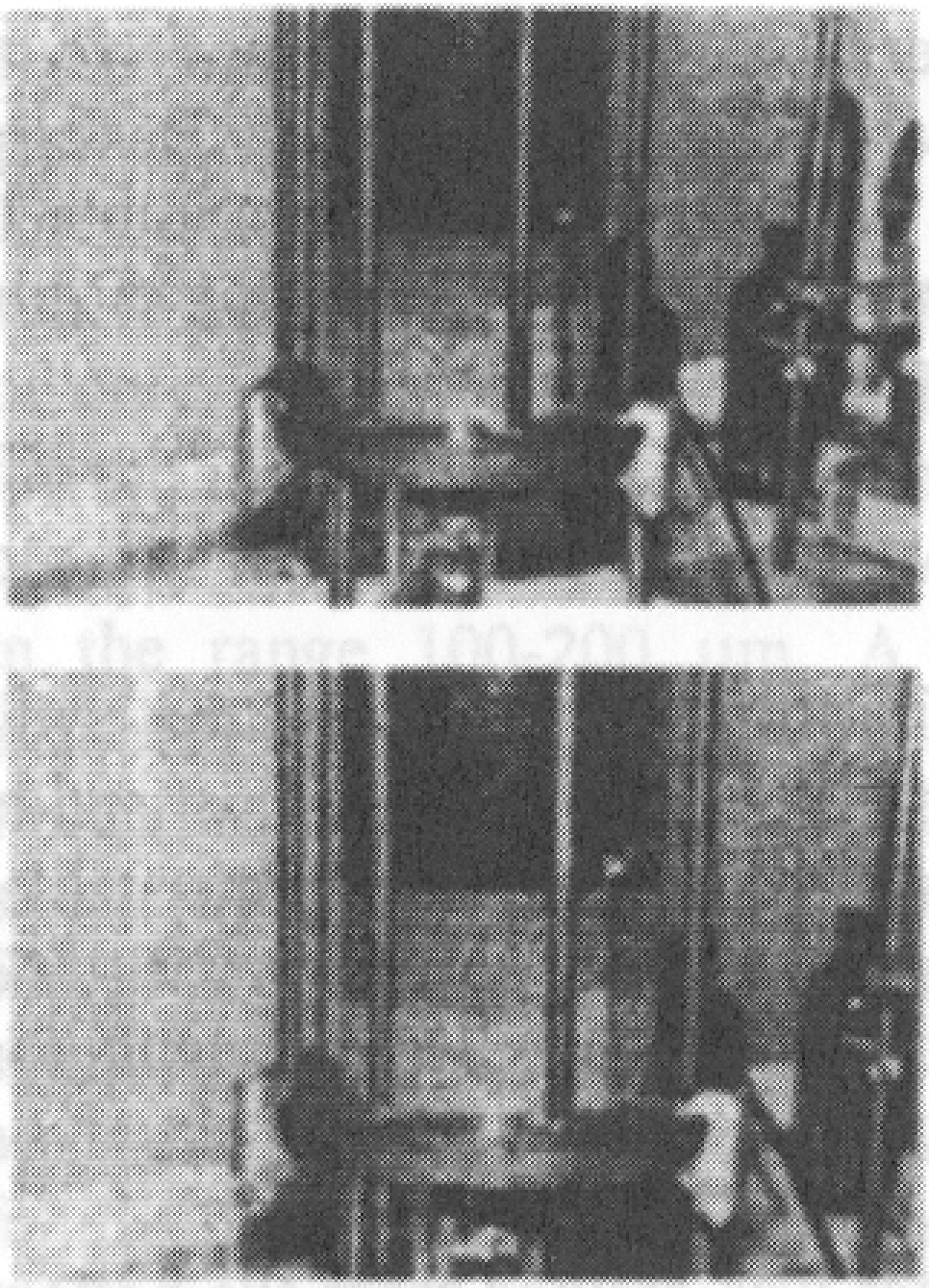

Figure 1. Flow front observation

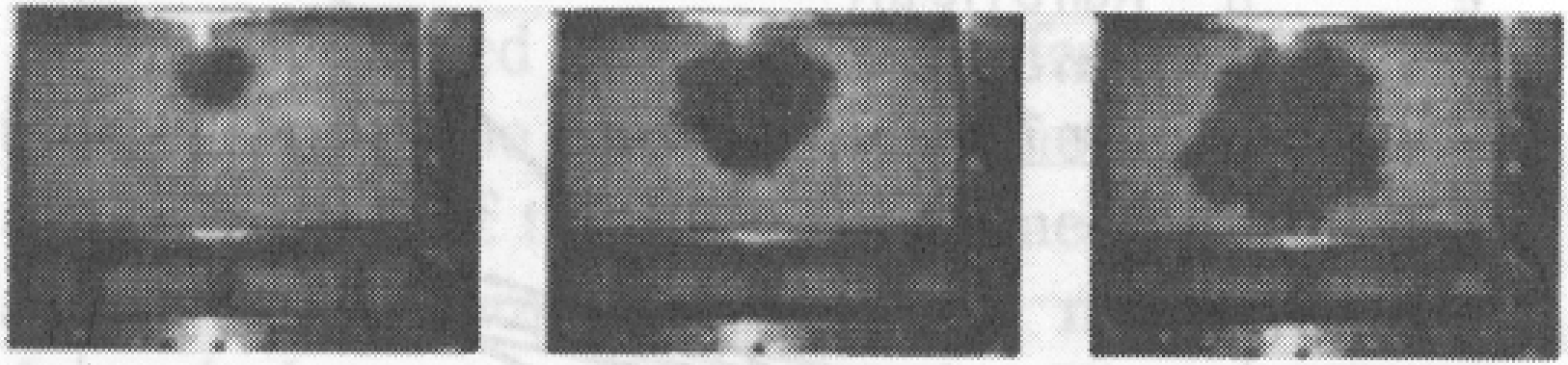

a) 88 sec. after DNAPL injection

b) 236 sec. after DNAPL injection

c) 604 sec. after DNAPL injection

Figure 4. Digital images showing DNAPL plume development in Run 2 with time.

Figure 6. Example of preferential boundary flow view from front window-side of model, and corresponding view from top of model excavated to 3.7 cm below surface.

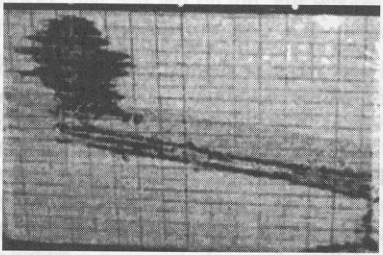

Figure 7: Photograph with the final pattern of the DNAPL plume at a similar 1-g experiment in an inclined layered saturated system (from Coumoulos et al, 1998).

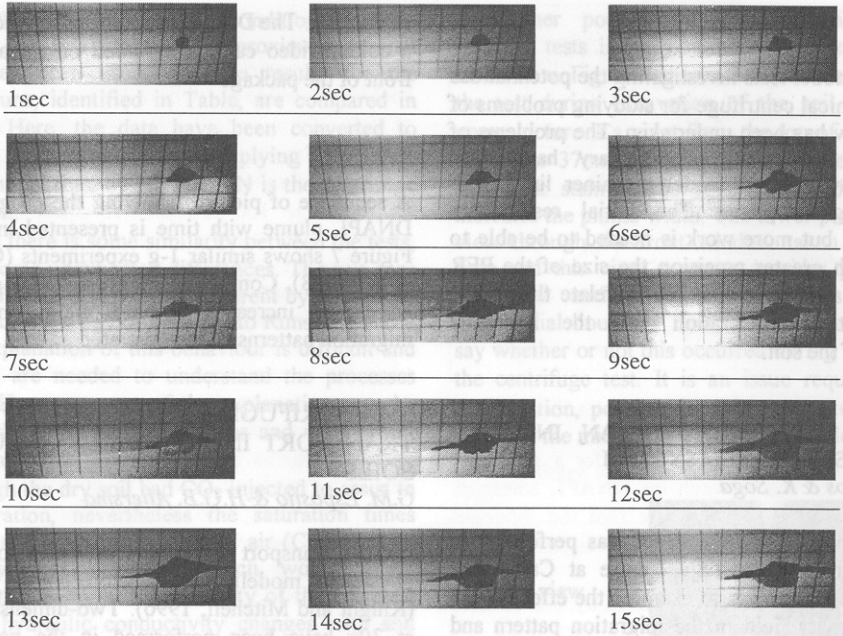

Figure 8. Photographs with location of the DNAPL plume at different times

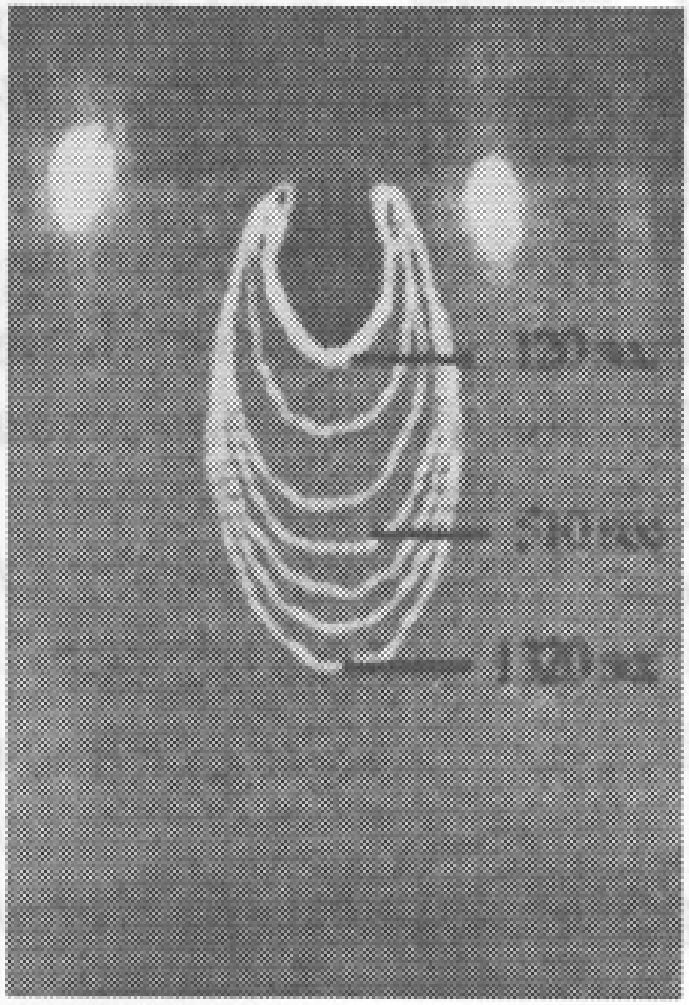

a

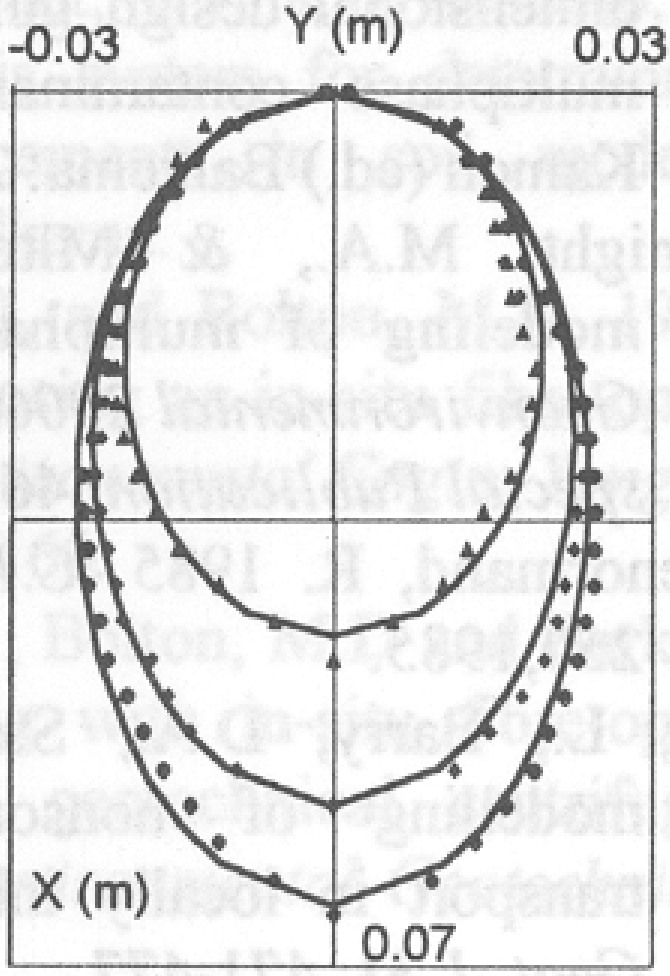

b

Figure 11. Picture (a) and fit (b) of the plumes in time (120, 510 and 1320 sec.).